

AD-752 509

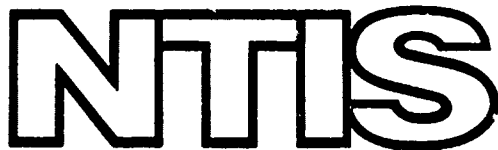
DETERMINING PRESENCE, THICKNESS, AND
ELECTRICAL PROPERTIES OF STRATIFIED MEDIA
USING SWEPT-FREQUENCY RADAR

Jerry R. Lundien

Army Engineer Waterways Experiment Station
Vicksburg, Mississippi

November 1972

DISTRIBUTED BY:



National Technical Information Service
U. S. DEPARTMENT OF COMMERCE
5285 Port Royal Road, Springfield Va. 22151

AB 752509

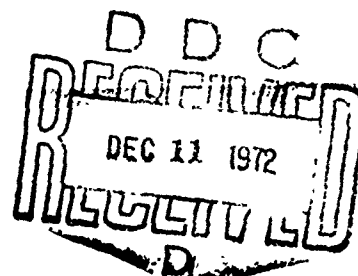


TECHNICAL REPORT M-72-4

DETERMINING PRESENCE, THICKNESS, AND ELECTRICAL PROPERTIES OF STRATIFIED MEDIA USING SWEPT-FREQUENCY RADAR

by

J. R. Lundien



NATIONAL TECHNICAL
INFORMATION SERVICE

November 1972

Sponsored by Office, Chief of Engineers, U. S. Army
and
U. S. Army Engineer Topographic Laboratories

Conducted by U. S. Army Engineer Waterways Experiment Station
Mobility and Environmental Systems Laboratory
Vicksburg, Mississippi

APPROVED FOR PUBLIC RELEASE; DISTRIBUTION UNLIMITED

67

**Destroy this report when no longer needed. Do not return
it to the originator.**

**The findings in this report are not to be construed as an official
Department of the Army position unless so designated
by other authorized documents.**

Unclassified

Security Classification

DOCUMENT CONTROL DATA - R & D

(Security classification of title, body of abstract and indexing annotation must be entered when the overall report is classified)

1. ORIGINATING ACTIVITY (Corporate author) U. S. Army Engineer Waterways Experiment Station Vicksburg, Mississippi		2a. REPORT SECURITY CLASSIFICATION Unclassified
		2b. GROUP
3. REPORT TITLE DETERMINING PRESENCE, THICKNESS, AND ELECTRICAL PROPERTIES OF STRATIFIED MEDIA USING SWEEP-FREQUENCY RADAR		
4. DESCRIPTIVE NOTES (Type of report and inclusive dates) Final report		
5. AUTHOR(S) (First name, middle initial, last name) Jerry R. Lundien		
6. REPORT DATE November 1972	7a. TOTAL NO. OF PAGES <i>67</i>	7b. NO. OF REFS 7
8a. CONTRACT OR GRANT NO.	9a. ORIGINATOR'S REPORT NUMBER(S) Technical Report M-72-4	
b. PROJECT NO. 4A061102B52E-01 4A062112A854-02	9b. OTHER REPORT NO(S) (Any other numbers that may be assigned this report)	
c.		
d.		
10. DISTRIBUTION STATEMENT Approved for public release; distribution unlimited.		
11. SUPPLEMENTARY NOTES	12. SPONSORING MILITARY ACTIVITY Office, Chief of Engineers, U. S. Army Washington, D. C., and U. S. Army Engineer Topographic Laboratories, Ft. Belvoir, Va.	
13. ABSTRACT The ability of a swept-frequency radar system operating under field conditions to detect the presence and measure the thickness of layered substrata and to determine the electrical properties of the materials in these substrata was studied. Reflectivity on sections of asphaltic concrete pavement structures (i.e. asphalt highway) of various subsurface layer thicknesses was measured by a specially designed microwave system operating over the frequency range of 0.25 to 8.0 GHz at perpendicular incidence. Test results indicated that swept-frequency radar measurements can be used to estimate power reflectance from the surface material of highway structures and to determine the amplitude of the subsurface contribution. Also, interference patterns, produced in the power reflectance curves, can be used to calculate the thickness of each layer of the structure.		

DD FORM 1 NOV 66 1473 REPLACES DD FORM 1473, 1 JAN 66, WHICH IS
OBSOLETE FOR ARMY USE.

Unclassified

Security Classification

I-A

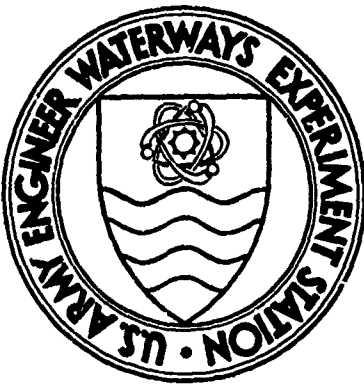
Unclassified
Security Classification

14 KEY WORDS	LINK A		LINK B		LINK C	
	ROLE	WT	ROLE	WT	ROLE	WT
Flexible pavements						
Microwaves						
Radar						
Reflectivity						
Stratified media						
Swept-frequency radar						

Unclassified

Security Classification

I-B



TECHNICAL REPORT M-72-4

DETERMINING PRESENCE, THICKNESS, AND ELECTRICAL PROPERTIES OF STRATIFIED MEDIA USING SWEPT-FREQUENCY RADAR

by

J. R. Lundien



November 1972

Sponsored by Office, Chief of Engineers, U. S. Army
Project No. 4A061102B52E-01

and

U. S. Army Engineer Topographic Laboratories
Project No. 4A062112A854-02

Conducted by U. S. Army Engineer Waterways Experiment Station
Mobility and Environmental Systems Laboratory
Vicksburg, Mississippi

ARMY-MRC VICKSBURG, MISS.

APPROVED FOR PUBLIC RELEASE; DISTRIBUTION UNLIMITED

I-C

FOREWORD

The study reported herein was conducted at the U. S. Army Engineer Waterways Experiment Station (WES) during the period 1970-1971. Guidance and funds for this work were provided by the Office, Chief of Engineers, under Military Engineering Research Project No. 4A061102B52E-01, and by the U. S. Army Engineer Topographic Laboratories under Military Geographic Analysis Project No. 4A062112A854-02.

The tests were performed by personnel of the Terrain Analysis Branch (TAB), Mobility and Environmental Systems Laboratory, under the general supervision of Messrs. W. G. Shockley and S. J. Knight, Chief and Assistant Chief, respectively, of the Mobility and Environmental Systems Laboratory; W. E. Grabau, Chief, TAB; and A. N. Williamson, Project Manager. Mr. J. R. Lundien directed the study with the assistance of Dr. H. Nikodem. Persons actively engaged in the program included Messrs. E. A. Baylot, J. R. Lundien, P. A. Smith, and J. H. Meeks and Miss Margaret H. Smith of TAB, and Mr. G. H. Jetton of the Instrumentation Services Division, WES. This report was written by Mr. Lundien.

Special acknowledgment is made to representatives of the Mississippi State Highway Department for their cooperation in providing test sites and highway design information for this test program.

COL Ernest D. Peixotto, CE, was Director of the WES during the conduct of this study and preparation of this report. Mr. F. R. Brown was Technical Director.

CONTENTS

	<u>Page</u>
FOREWORD	iii
NOTATION	vii
CONVERSION FACTORS, BRITISH TO METRIC AND METRIC TO BRITISH UNITS OF MEASUREMENT	ix
SUMMARY	xi
PART I: INTRODUCTION	1
Background	1
Previous WES Investigations	2
Purpose and Scope of Test Program	3
Definitions of Pertinent Terms	3
PART II: TEST PROGRAM	5
Swept-Frequency Radar System	5
Test Sites	10
Reference Standard	13
Test Procedures	14
Test Results	17
PART III: REDUCTION AND ANALYSIS OF DATA	19
Target Model	19
Spectral Response	20
Spectral Analysis	21
Discussion of Results	31
PART IV: CONCLUSIONS AND RECOMMENDATIONS	38
Conclusions	38
Recommendations	38
LITERATURE CITED	40
TABLES 1 and 2	
PLATES 1-12	
APPENDIX A: FOURIER TRANSFORM ANALYSIS	

NOTATION

c	Velocity of electromagnetic wave through free space, m/sec
d	Layer thickness, m
e	Base of natural logarithm
E	Electric field intensity, v/m
E_i	Incident electric field intensity, v/m
E_o	Reference electric field intensity, v/m
E_r	Reflected electric field intensity, v/m
f	Frequency, Hz
j	$\sqrt{-1}$
n	Harmonic number
P_{RR}	Reflected power from the reference standard, w
P_{RS}	Reflected power from the test site, w
P_{TR}	Transmitted power with the reference standard in place, w
P_{TS}	Transmitted power with the test site exposed, w
r	Electric wave reflectance
R	Power reflection coefficient
R_\perp	Power reflection coefficient for perpendicular polarization
R_{\parallel}	Power reflection coefficient for parallel polarization
t	Time, sec
T_f	Oscillation period, Hz
x	Distance, m
Z	Impedance, ohms
α	Attenuation constant, m^{-1}
β	Phase constant, m^{-1}
γ	Propagation factor, m^{-1}
ϵ	Dielectric constant, F/m

ϵ_0	Dielectric constant of free space, F/m
ϵ_r	Relative dielectric constant, dimensionless
θ	Angle of incidence, deg
λ	Wavelength, m
μ	Magnetic permeability, H/m
μ_0	Magnetic permeability of free space, H/m
μ_r	Relative magnetic permeability, dimensionless
σ	Conductivity, mhos/m
ω	Circular frequency, radians/sec

CONVERSION FACTORS, BRITISH TO METRIC AND
METRIC TO BRITISH UNITS OF MEASUREMENT

British units of measurement used in this report can be converted to metric units as follows:

<u>Multiply</u>	<u>By</u>	<u>To Obtain</u>
Fahrenheit degrees	5/9	Celsius or Kelvin degrees*
inches	2.54	centimeters

Metric units can be converted to British units as follows:

<u>Multiply</u>	<u>By</u>	<u>To Obtain</u>
meters	3.2808	feet
grams per cubic centimeter	62.43	pounds per cubic foot
centimeters	0.3937	inches
millimeters	0.03937	inches

* To obtain Celsius (C) temperature readings from Fahrenheit (F) readings, use the following formula: $C = (5/9)(F - 32)$. To obtain Kelvin (K) readings, use: $K = (5/9)(F - 32) + 273.15$.

DETERMINING PRESENCE, THICKNESS, AND ELECTRICAL PROPERTIES
OF STRATIFIED MEDIA USING SWEPT-FREQUENCY RADAR

PART I: INTRODUCTION

Background

1. Quantitative information on surface and subsurface materials is used for a variety of purposes: vehicle performance or foundation design strength can be predicted if the properties of the soil or rock involved are known; and the carrying capacities of pavements and other artificial surfaces can be evaluated if the strength of the medium, layer thicknesses, foundation properties, etc., can be determined. The nature and extent of the sampling and testing program necessary to acquire this information must be determined by means of the following criteria: (a) what information is required; (b) how the information is extracted from measurements; and (c) the cost and time involved in gathering the information.

2. Test programs are classified as either destructive or nondestructive, depending on the method of measurement. In a destructive program, samples are removed at specific points (usually widely spaced) and are tested at the site or in the laboratory. This type of program can be very quick and cheap or very time-consuming and expensive, depending on the information required and the material being sampled.

3. Nondestructive testing allows the user to look at a large portion of an area, usually more quickly than in destructive testing, and does not require the removal of any material. However, the equipment used for nondestructive testing is quite expensive, and the data collected are difficult to interpret. For example, seismic surveys are used to obtain acceptably accurate measurements of layering in many situations, but detection of an interface between two layers is difficult or impossible if a high-propagation-velocity material overlies a low-propagation-velocity material. Although this situation does not ordinarily occur in natural soils, it is almost invariably present in

artificial media, such as pavements.

4. The above-mentioned considerations led to the idea that measurements made with microwave energy might provide an acceptable solution to the problem of nondestructive testing of layered media such as soils and rocks. Microwave energy can penetrate most terrain materials to some degree and is sensitive to changes in the electrical properties of these materials. In addition to being nondestructive, microwave systems are noncontact devices, a fact which allows a wide variety of mounting options ranging from air platforms to surface vehicles.

5. Deep sensing through ice with radar systems operating at high frequencies has been perfected. Results of such sensing operations show layers within the ice (i.e. changes in ice density due to age) as well as the total ice depth. Shallow sensing with these devices is not feasible because of low resolution; also, the transmitted signal interferes with the near-surface return (i.e. the duration of the transmitted pulse is too long).

6. Sensing through soils or other terrain materials demands the use of low frequencies to achieve penetration. In general, the lower the frequency, the less attenuation the wave experiences when traveling in a given material. The duration of the transmitted pulse must be kept short to provide an acceptable degree of resolution or time discrimination when thicknesses of thin layers are measured. Systems with extremely short pulses (monopulse systems) operating at low frequencies have not been used very successfully because of data interpretation problems associated with antenna propagation (ringing and dispersion).

7. Swept-frequency radar can provide an acceptable depth of penetration into terrain materials when the transmitter is operating at low radar frequencies. Pulse width and distortion problems are eliminated by operating in a continuous wave mode. Surface and subsurface information can then be extracted through interpretation of interference patterns found in the reflectance data.

Previous WES Investigations

8. Several investigations with microwave systems have already been

conducted at the U. S. Army Engineer Waterways Experiment Station (WES) and the results have been published. These investigations included a laboratory study to examine the possible use of pulsed radar systems to detect and measure the depths of surface water and groundwater and changes in soil moisture contents,^{1,2} and a laboratory study with a microwave interferometer that measured the basic electrical properties of various test samples and related these properties to the physical properties of the test sample.³ The results of these studies showed that: (a) the electrical properties of soils and other materials can be measured remotely (the range used in the radar study was approximately 14 m*), (b) there is a direct correlation between a soil's dielectric constant and water content, and (c) long-wavelength microwave energy will penetrate to and reflect from subsurface interfaces.

Purpose and Scope of Test Program

9. The purpose of the overall research program was to develop methods for extracting quantitative information from terrain surfaces through use of specially designed microwave systems. The specific objective of this study was to determine the ability of a swept-frequency radar system operating under field conditions to: (a) detect the presence of substrata of various thickness, densities, and composition; and (b) develop analytical procedures for extracting, from the reflectance curves, information related to the electrical properties of the materials in these substrata.

Definitions of Pertinent Terms

10. Certain terms used in this report are defined as follows:

Attenuator. A device that reduces the amplitude of an electrical signal without introducing appreciable phase or frequency distortion.

* A table of factors for converting British units of measurement to metric units and metric units of measurement to British units is presented on page ix.

Bandwidth. The difference between the limiting frequencies of a continuous frequency band. The bandwidth of a device is the difference between limiting frequencies where performance falls within specified limits.

Conductivity. The electrical conductance of a material having unit length and unit cross section.

Dielectric constant. That property of a material that determines the electrostatic energy stored per unit volume for unit potential gradient; synonymous with permittivity.

Directional coupler. A device that divides the input signal into two output signals. Both output signals, one being much larger than the other, are proportional to the input signal.

Incidence angle. The angle between the line normal to the surface at the point of incidence of the electromagnetic wave and the line of propagation of the wave to the surface.

Isolator. A device used to minimize the coupling or interaction of components.

L-band: A range of frequencies from 0.39 to 1.5 GHz.

Loss tangent. The relation between the dielectric constant and conductivity at a given frequency; synonymous with dissipation factor.

Microwaves. Radio waves that have wavelengths so short that they exhibit some of the properties of light.

Octave. The interval between two frequencies having a ratio of two to one.

Optical thickness. The distance separating two reflecting surfaces in free space that would give the same displacement measurement as that obtained from the two surfaces of a dielectric layer.

Polarization. A term used to specify the direction of the electric vector in a polarized radio wave with respect to the direction of propagation.

Power reflection coefficient. The ratio of the reflected power density at the surface of a material to the incident power density.

PART II: TEST PROGRAM

Swept-Frequency Radar System

11. The swept-frequency radar system used in this investigation (fig. 1) was designed to measure reflectance from a test site over the frequency range of 0.25 to 8.0 GHz. The system, which can be moved from site to site on three vehicles, is composed of two major sub-assemblies, i.e. the transmitter and the receiver system.

12. The transmitter section generates a signal directed at the test site. The portion of the signal reflected by the test site and collected at the receiver antenna is processed through the receiver's electronic circuits to a recorder.

13. The principal components of the swept-frequency radar system are shown in fig. 2. Details are presented in the following paragraphs on how the various functions are performed.

The heart of the transmitter section is the



Fig. 1. Truck-mounted swept-frequency radar system

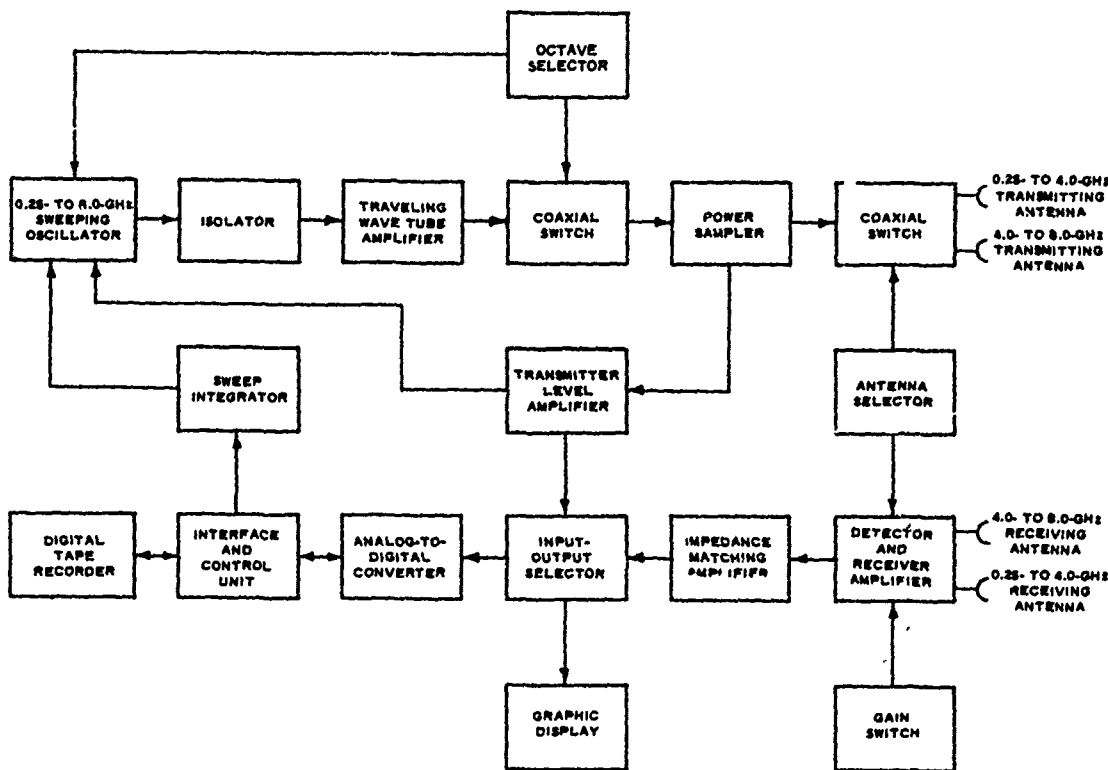


Fig. 2. Swept-frequency radar block diagram

0.25- to 8.0-GHz sweeping oscillator. On command, it generates frequencies over octave bands (sweeping one octave at a time) at selected power levels. The rated power output for each octave is shown in the following tabulation:

Frequency Range, GHz	Rated Power Output milliwatts
0.25 - 0.5	20
0.5 - 1.0	50
1.0 - 2.0	60
2.0 - 4.0	50
4.0 - 8.0	25

The rate of frequency change can be controlled by means of an external signal. The output power can be leveled by sampling a portion of the transmitted power at a control point and routing a d-c voltage

proportional to the sampled power back to the sampling input on the sweeping oscillator.

14. The 0.5- to 8.0-GHz signals generated by the sweeping oscillator are routed to the appropriate traveling wave tube amplifier through an isolator (10-db attenuator). The 0.25- to 0.5-GHz signals need no further amplification, since attenuation through the various components is low at these frequencies. Traveling wave tube amplifiers are used because of their relatively wide bandwidth and uniform gain characteristics; the minimum rated gain and rated power output are given below:

Frequency GHz	Minimum Rated Gain db	Rated Power Output W
0.5 - 1.0	30	1.0
1.0 - 2.0	20	10.0
2.0 - 4.0	30	10.0
4.0 - 8.0	30	10.0

Isolators are used between the sweeping oscillator and the traveling wave tube amplifiers to adjust the power levels to the best range of operation and to reduce interaction between the two components.

15. The signals are routed from the traveling wave tube amplifier (or directly from the sweeping oscillator in the case of the 0.25- to 0.5-GHz octave) through the single transmitter coaxial cable to a coaxial switch. The coaxial switch, controlled by the octave selector, directs the signals to the proper power sampler (i.e. one of five directional couplers).

16. The power sampler divides the input power into two components, one much larger than the other. The smaller component, proportional to the signal applied to the transmitting antennas, is rectified with a crystal detector and routed to the transmitter level amplifier. Two outputs are obtained from this amplifier; one is available for recording in the receiver section, and the other is fed back to the leveling input on the sweeping oscillator to keep the transmitted power at a constant level.

17. The larger output from the power sampler is the signal applied to the transmitter antenna. A coaxial switch controlled by the antenna selector connects the proper power sampler to the 0.25- to 4.0-GHz transmitting antenna. The 4.0- to 8.0-GHz transmitting antenna remains connected to the 4.0- to 8.0-GHz power sampler at all times.

18. Two parabolic transmitting antennas are used to propagate the frequencies generated in the transmitter section through space toward the boresighted center of the top surface of the test site. The two antennas have the following characteristics:

	0.25- to 4.0-GHz Antenna	4.0- to 8.0-GHz Antenna
Antenna diameter, m	1.83	0.71
Antenna polarization	Linear	Linear
Antenna feed	Log periodic	Wave guide horn
Half-power beam width, deg, at:		
0.3 GHz	31	--
2.5 GHz	5	--
5.0 GHz	--	7
7.0 GHz	--	5
Antenna gain (over an iso- tropic radiator), db, at:		
0.3 GHz	14	--
2.5 GHz	30	--
5.0 GHz	--	27
7.0 GHz	--	30

19. Two parabolic receiving antennas are used to collect a portion of the microwave energy reflected from the test site. They are identical with the two transmitting antennas and are also boresighted toward the center of the top surface of the test site.

20. Through the application of the antenna selector switch, the signal from the proper receiving antenna is rectified with a crystal detector and amplified in the receiver amplifier. The amplifier gain is controlled with a gain switch and has four ranges: 0-30, 0-100, 0-300, and 0-1000 μ w.

21. The receiver signal is sent to the impedance matching amplifier, which reduces the source impedance and scales the amplitudes for further processing.

22. The input-output selector is used to select either the receiver signal from the impedance matching amplifier or the transmitter signal from the transmitter level amplifier. The selected signal is then routed either to an x-y recorder for a graphic display or to the analog-to-digital (A-D) converter for further processing. An oscilloscope is also used to monitor the input signal at this point.

23. The A-D converter digitizes the input signal at a 200-character-per-second rate on command from the interface and control unit. The digitizing rate is well within the capability of the A-D converter (bandwidth in excess of 100,000 Hz) and is fast enough to stop power fluctuations caused by antenna movement. The output, a 12-bit binary number, is fed to the interface and control unit.

24. The interface and control unit prepares the digital signal for recording on the digital tape recorder. The recorder has two modes of operation:

- a. A fixed data mode, in which data from 12 thumb wheel switches can be recorded on the tape.
- b. An external data mode, in which the data from the analog-to-digital-converter can be recorded.

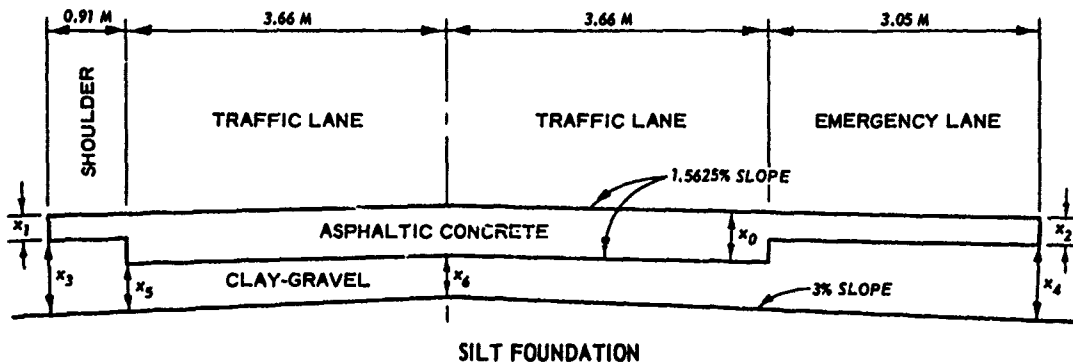
The fixed data mode permits identification (site number, octave frequency band, receiver gain setting, transmitter or receiver power recording, and sample or reference standard recording) of the external data. In the external data mode, 256 data words are recorded for each frequency octave. The use of 256 data words per octave was adequate to resolve the highest frequencies of interest in the data record. In addition, each time a digital word is recorded, a signal is sent from the interface and control unit to the sweep integrator.

25. The sweep integrator conditions the pulse from the interface and control unit and applies the resulting signal to an integrator circuit. The output is a ramp voltage (an analog signal) that starts at

zero volts and increases an equal amount each time the signal is digitized and recorded. This ramp voltage is fed back to the sweeping oscillator for frequency control. The generated frequency is lowest when the ramp voltage is zero and increases to twice the lowest frequency (one octave) at the highest ramp voltage.

Test Sites

26. Three sites on Interstate Highway 20 near Clinton, Miss. were selected for tests with the swept-frequency radar system. The highway was constructed on a silt foundation and, at the time of the tests, had an 8.5-in. asphaltic concrete surface (final design thickness of the asphaltic concrete was 11 in.). The pavement was separated from the silt foundation by a clay-gravel base course. The profile of a typical highway section is shown in fig. 3, and the highway data are given in table 1. A summary of the soils data collected by



NOTE: VALUES FOR x ARE GIVEN IN TABLE 1.

Fig. 3. Highway profile for westbound traffic (not to scale)

the Mississippi State Highway Department in the vicinity of the test sites is given below:

- a. Clay-gravel base. This granular material had from 10 to 26 percent fines (silt- and clay-sized particles passing a No. 200 sieve) and from 35 to 48 percent gravel (material retained on a No. 4 sieve). It classified SP-SC to SM according to the Unified Soil Classification System (USCS). The Atterberg limits for material passing a No. 40 sieve were: liquid limit, 18-23; and plasticity index, 4-9 (some samples were nonplastic).

b. Silt foundation. This fine-grained material (99 percent fines) at site 1 (sta 724) and site 2 (sta 654) classified CI according to the USCS. Its average Atterberg limits were: liquid limit, 33; and plasticity index, 14. At site 3 (sta 604) the soil had less clay (96 percent fines) and classified CL-ML. Its average Atterberg limits were: liquid limit, 28; and plasticity index, 6. At site 1 the finish grade was the natural soil; at site 2 approximately 1 m of fill was placed over a 1-m-high by 1.5-m-wide concrete box culvert; and at site 3 approximately 0.6 m of fill was placed to attain roadbed elevation. The fill materials were the same as the silt foundation except for being reworked and compacted.

27. The moisture contents and dry densities of the foundation materials varied from point to point along the highway. For example, at site 1 (sta 724), during highway construction, the moisture content and dry density of the clay-gravel base were 4.4 percent and 2.04 g/cm^3 , respectively. Moisture content in nearby sample points ranged from 3.8 to 7 percent, and dry density from 1.94 to 2.17 g/cm^3 . The variations were similar for the silt foundation; the moisture content ranged from 20 to 25 percent, and the dry densities from 1.52 to 1.81 g/cm^3 . These same variation ranges also were noted at sites 2 and 3.

28. Because of the above-mentioned variations in density and moisture content, a single relative dielectric constant value (necessary for later analysis of data) was chosen for each highway material. These dielectric constants were representative of the length of highway on which tests were made. The constants were obtained from curves of relative dielectric constant versus water content, determined from previous laboratory investigations at the WES.³ Two such curves, shown in fig. 4, represent data obtained from 414 samples of sands, silts, and clays (actually 12 different soils).

29. For the clay-gravel base, a moisture content of 5 percent and a dry density of 2 g/cm^3 were selected. These are equivalent to a water content of 0.1 g/cm^3 (the product of moisture content and dry density), resulting in a relative dielectric constant of 6.5 (from fig. 4). For the silt foundation, a moisture content of 19 percent and a dry density of 1.6 g/cm^3 were selected. These are equivalent to a water content of

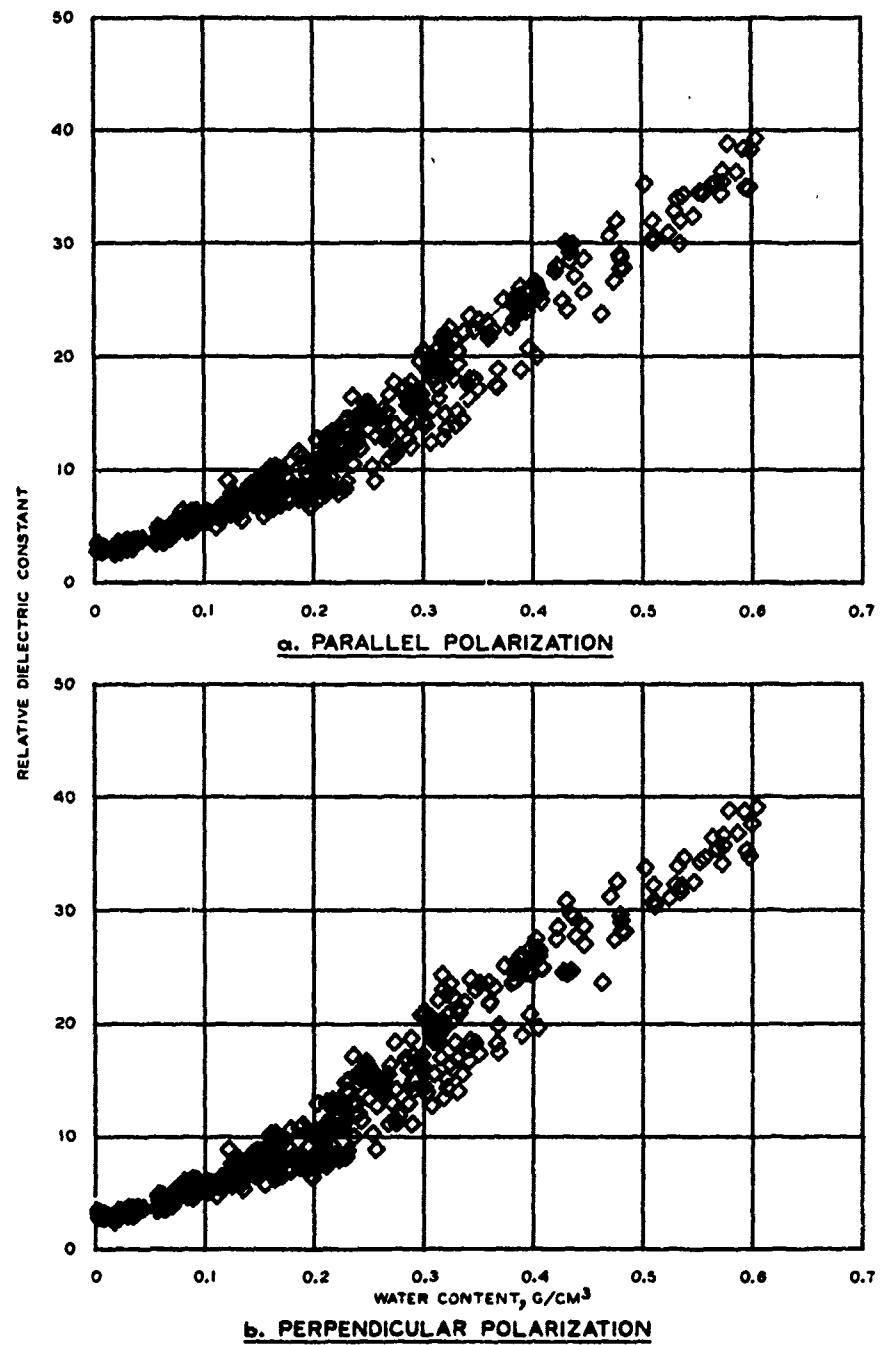


Fig. 4. Effect of water content on the relative dielectric constant of soils at a frequency of 1.074 GHz

0.3 g/cm³, resulting in a relative dielectric constant of approximately 16. The electrical properties of the asphaltic concrete were obtained from laboratory measurements with an L-band interferometer on specially prepared 84-cm-square by 5-cm-deep samples of coarse asphaltic concrete (coarse aggregate that can pass through a 1-1/2-in. screen). This sampled material was identical with the asphaltic concrete at the highway sites; for the laboratory tests, the angle of incidence was 45 deg (fixed by interferometer design) and the temperature was 24 C, or room temperature. A relative dielectric constant of 3.53 was selected for this material. The measured electrical properties are given in the tabulation below:

Frequency GHz	Polarization	Relative Dielectric Constant	Loss Tangent	Conduc- tivity mho/m
1.074	Parallel	3.55	0.024	0.005
	Perpendicular	3.55	0.038	0.008
1.124	Parallel	3.49	0.013	0.003
	Perpendicular	3.58	0.032	0.007
1.311	Parallel	3.47	0.021	0.005
	Perpendicular	3.52	0.049	0.012
1.412	Parallel	3.51	0.009	0.002
	Perpendicular	3.52	0.048	0.008
1.490	Parallel	3.54	0.013	0.004
	Perpendicular	3.52	0.025	0.007

Reference Standard

30. The reflected signal from a reference standard was measured prior to each highway measurement. Any changes in system operation showed up as changes in both measurements and were canceled when the power reflectance was calculated (see paragraph 35).

31. The reference standard was constructed of metal plates supported on a metal frame in a fold-up design (fig. 5) that made the standard portable. Because the high-conductivity metal made a microwave mirror, nearly all the incident power was reflected (or reradiated) specularly.

32. When set up, the reference standard measured 3.35 m square.

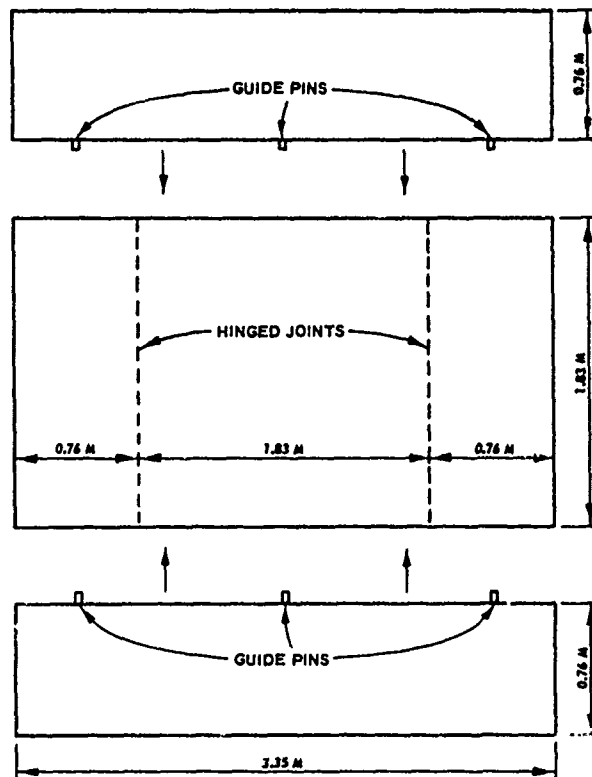


Fig. 5. Reference standard

There was no middle seam in the metal plate to interfere with reflectance measurements made when the antenna beam widths were small. When the antenna beam widths were large, there were four seams in the illuminated area. However, since the seam area was small compared with the total illuminated area, there was very little effect on the total reflected signal.

Test Procedures

33. It was important that each swept-frequency radar test be performed in an identical fashion so that variations in the data would be caused by the reflectance variations of the test site alone. Procedures were developed to insure that the relative positions of the antennas with respect to the reference standard (when in place) would remain the same even though the equipment was moved from site to site. These procedures are described in the following paragraphs.

34. The midpoint between the transmitting and receiving antennas was positioned directly above the test site. The antennas were rotated with electric motors about the midpoint until they were in a horizontal plane, and the plane formed by the lines of boresight was vertical. This leveling procedure was checked with level lights controlled by mercury switches that turned on when the antennas were in proper alignment. The range (the vertical height of the antenna carriage minus the distance the antennas were mounted below the carriage) used for these tests was 7.6 m. The reference standard was moved to the center of the test site and leveled by using a bubble level at each corner. The position of the reference standard in the center of the test site was checked with a closed-circuit television system, the camera of which was mounted at the midpoint between the transmitting and receiving antennas on the antenna carriage in boresight with the antennas. The position and height of the antennas were also checked with a weighted line connected at the same point as the television camera midway between the transmitting and receiving antennas.

35. The transmitter and receiver sections of the system were energized, and the transmitted power and the power reflected by the reference standard to the receiving antenna as the frequency was varied were recorded. Although the power applied to the antennas was maintained at a constant value over each octave band (see paragraph 16), the antennas were not uniformly efficient at all frequencies, and the power collected by the receiving antennas from the reference standard varied in amplitude (fig. 6). The reference standard was then removed, exposing the surface of the test site. The transmitted and received power were again recorded. The sample power reflectance referenced to the standard reflectance was calculated for all frequencies as:

$$R = \frac{P_{RS}/P_{TS}}{P_{RR}/P_{TR}} = \frac{P_{RS} P_{TR}}{P_{RR} P_{TS}} \quad (1)$$

where

R = power reflection coefficient

P_{RS} = reflected power from the test site, w

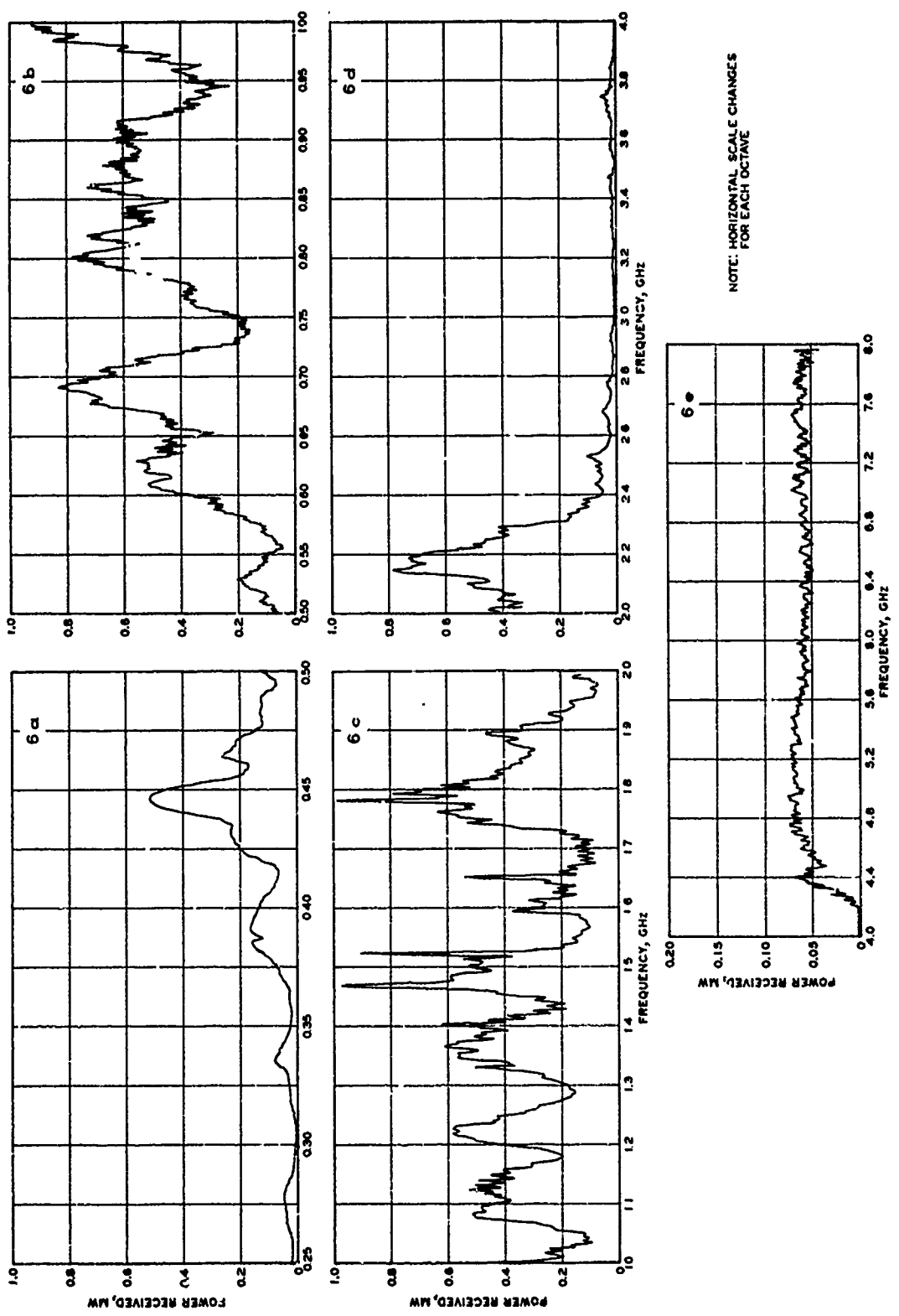


Fig. 6. Reflected power from reference standard

P_{TS} = transmitted power with the test site exposed, w

P_{RR} = reflected power from the referenced standard, w

P_{TR} = transmitted power with the reference standard in place, w

36. Three replicate tests were made at each test site. The data, in terms of power reflectance, were then used for layer analysis and for the calculation of electrical properties (see paragraphs 60-69).

Test Results

37. The curves of power reflectance versus frequency are given in plates 1-3 for site 1, plates 4-6 for site 2, and plates 7-9 for site 3. Each of these curves was developed by applying equation 1 to the data obtained from the four separate recordings of transmitted and received power for both the reference standard and the test site.

38. The accuracy of the measured data must be considered to be better at some frequencies than at others. For example, the beam of the transmitting and receiving antennas at the lowest operating frequencies (around 0.25 GHz) was wide enough at a height of 7.6 m to allow part of the projected beam to fall outside the reference standard. Also, the antennas used in this system had limited bandwidths. The low-frequency antennas had a specified bandwidth of 0.3 to 3.0 GHz, and the high-frequency antennas had a bandwidth of approximately 4.5 to 8.0 GHz. Microwave energy outside these frequency ranges was not handled efficiently, as shown by the extremely low amplitudes recorded for these points in fig. 6. Arithmetic operations on such data tend to have a higher percentage of error associated with each calculation than those on data inside the antenna bandwidths. For these reasons, analysis was concentrated on data in the 0.5- to 2.0-GHz frequency region. The 4.5- to 8.0-GHz frequency region provided information on surface and near-surface properties because of its lesser penetrating power. The 0.25- to 0.5-GHz frequency region had the highest penetrating power, but was used only to check for trends because of the errors discussed

above. Information in the 2.0- to 8.0-GHz frequency region was found to be insufficiently accurate for measuring the sample properties.*

* The data obtained in the 4.0- to 8.0-GHz band appear to be out of calibration by 200 to 300 percent when compared with the data in the 0.5- to 2.0-GHz bands.

PART III: REDUCTION AND ANALYSIS OF DATA

Target Model

39. When an electromagnetic wave traveling in one medium impinges upon a second medium having differing electrical properties, the wave generally will be partially transmitted and partially reflected. The transmitted wave is attenuated as it travels through the second medium and, upon encountering a third medium, experiences partial reflection and transmission again. Theoretically, this process can continue indefinitely. The reflected signals of interest are those that travel back to the surface with enough amplitude to significantly alter the total amplitude of the return signal. The amplitudes of the reflected signals are governed by the properties of the medium. Certain assumptions were made regarding these properties in order to simplify the methods used to extract information about the medium from the reflection curves, as discussed below.

40. The test sites were assumed to be composed of layers of various thicknesses. The material in each layer was uniform and did not have any discontinuities either within the layer or at its top and bottom surfaces. The electrical properties of each material were assumed to be frequency independent (at least over the frequency range used for calculations) and predictable from past tests in the laboratory.

41. The transition zones between the layers were assumed to be very thin (negligible) and, thus, the layer interfaces abrupt. A thick transition zone would tend to reduce the amplitude of the boundary reflection and might cause a layer to be overlooked. This is a matter of degree, since the thickness is measured relative to the wavelength of the transmitted signal in the material through which the wave is traveling. A thin transition zone at long wavelengths might be a very thick transition zone at short wavelengths. For the purpose of this report, a thin transition zone is one whose thickness is less than one-eighth of a wavelength of the transmitted signal (Rayleigh criterion).

42. Each layer surface was assumed to be smooth. Again, smoothness is a matter of degree and can be evaluated by comparing the surface

roughness deviations to one-eighth of a wavelength of the transmitted signal in the same manner as that for the transition zones. The assumption for smoothness allows prediction of surface electrical properties, since, in general, roughness tends to reduce the signal level at the radar receiver by scattering the reflected energy and thus tends to decrease the accuracy of the computations.

43. In addition, the top and bottom surfaces of each layer were assumed to be parallel and perpendicular to the radar beam. If the layers were not parallel, the layer thickness would not be uniform. Also, a sloped surface would tend to direct the reflected energy away from the receiver and thus reduce the amplitude of that signal component.

44. These assumptions do not restrict operation to only ideal test sites; rather, the accuracy of computed results is increased when the assumptions are met.

Spectral Response

45. The reflectance of a material can be highly dependent on the frequency of the microwave source. Materials are roughly divided into two classes: (a) conductors and (b) dielectrics, or insulators. The dividing line between the two classes is not sharp, and some materials (soil, for example) are considered to be conductors in one part of the radio frequency range and dielectrics in another part. The criterion for classifications is the value of

$$\frac{\sigma}{\omega\epsilon}$$

where

σ = electrical conductivity, mhos/m

ω = circular frequency ($= 2\pi f$), radians/sec

f = frequency, Hz

ϵ = dielectric constant, farads/m

When $\sigma/\omega\epsilon$ (which is also defined as the ratio of conduction current density to displacement current density in the material) is greater

than 1, the material is a conductor, and when $\sigma/\omega\epsilon$ is less than 1, the material is a dielectric. At high frequencies (i.e. above a few megahertz), most nonmetallic terrain materials act as dielectrics insofar as their reflecting properties are concerned. The waves transmitted through the surface into the material are, however, rapidly attenuated.

46. The measurements discussed in this report were made at high frequencies (0.25 to 8.0 GHz) and, therefore, the materials are considered to be dielectrics, or poor conductors. For these materials (especially low-loss materials), energy penetration is possible, and reflection from subsurface layers can combine with surface reflections to give a total amplitude highly dependent on the layer geometry and transmitter frequency. Thus, a measurement at a single frequency cannot be used to predict the surface reflectance unless the test site is known to be without layers.

47. In general, the reflectance from an unlayered test site will change with increasing frequency because of the decreasing conductivity effect. Thus, in some cases, electrical properties can be predicted by making measurements at two frequencies, one much lower than the other, and noting the change in measurement amplitudes. This is not possible for most field measurements since test sites usually have some degree of layering.

48. For layered test sites, subsurface reflection can combine with the surface reflection to produce a periodic amplitude change as the frequency is varied. This amplitude change is caused by destructive and constructive wave interference and decays with increasing depth. In the case of field measurements, some scattering occurs from rough surfaces and in the transition zones between subsurface layers. This scattering reduces the influence of multiple-reflected waves. The net result, an increase in the noise level of the reflected signal, gives a somewhat random appearance to the reflectance curves.

Spectral Analysis

49. The following analysis outlines the derivation of the

equations used to reduce the swept-frequency radar data. A plane wave incident at an angle θ , with the normal to the plane boundary between two low-loss media (see fig. 7), will be reflected at an angle θ .

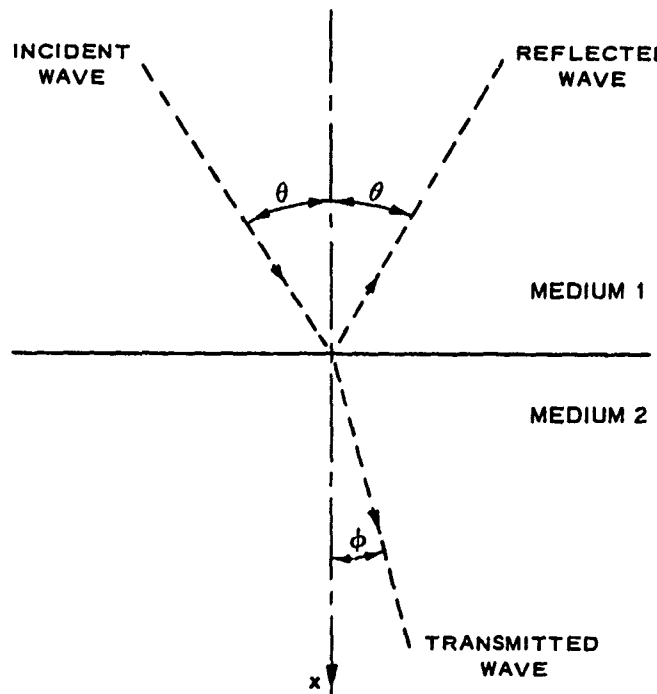


Fig. 7. Oblique incidence on boundary between two media

The equations for the reflection coefficients are given below.⁴ The expression for the electric field in medium 2 is

$$E = E_0 e^{j\omega t - \gamma x} \quad (2)$$

where

E = electric field intensity in medium 2, v/m

E_0 = reference electric field intensity, v/m

e = base of natural logarithm

$j = \sqrt{-1}$

t = time, sec

γ = propagation factor ($\gamma = \alpha + j\beta$), m^{-1}

x = distance measured in direction of propagation, m

α = attenuation constant, m^{-1}

β = phase constant, m^{-1}

The propagation factor can be computed from

$$\gamma = \sqrt{j\omega\mu(\sigma + j\omega\epsilon)} \quad (3)$$

where

μ = magnetic permeability ($\mu = \mu_r \mu_0$), H/m

ϵ = dielectric constant ($\epsilon = \epsilon_r \epsilon_0$), farads/m

μ_r = relative magnetic permeability, dimensionless

μ_0 = free space magnetic permeability, $4\pi \times 10^{-7}$ H/m

ϵ_r = relative dielectric constant, dimensionless

ϵ_0 = free space dielectric constant, $1/(36\pi \times 10^9)$, farads/m

The attenuation constant α is equal to the real part of the propagation factor:

$$\alpha = \omega \sqrt{\frac{\mu\epsilon}{2}} \left(\sqrt{1 + \frac{\sigma^2}{\omega^2\epsilon^2}} - 1 \right) \quad (4)$$

The phase constant β is equal to the imaginary part of the propagation factor:

$$\beta = \omega \sqrt{\frac{\mu\epsilon}{2}} \left(\sqrt{1 + \frac{\sigma^2}{\omega^2\epsilon^2}} + 1 \right) \quad (5)$$

For wave propagation in low-loss and nonmagnetic media

$$\frac{\sigma^2}{\omega^2\epsilon^2} \ll 1, \quad \sqrt{1 + \frac{\sigma^2}{\omega^2\epsilon^2}} \approx \left(1 + \frac{\sigma^2}{2\omega^2\epsilon^2} \right)$$

and

$$\alpha \approx \frac{\sigma}{2} \sqrt{\frac{\mu_0}{\epsilon}} = \frac{188.3\sigma}{\sqrt{\epsilon_r}} \quad (6)$$

$$\beta \approx \omega \sqrt{\mu_0 \epsilon} = \frac{2\pi f}{c} \sqrt{\epsilon_r} \quad (7)$$

where

c = free-space wave velocity, 300×10^6 m/sec.

50. If the frequency is sufficiently high, $\beta \gg \alpha$. The power reflections can be simplified from the more general expression found in the literature (see, for example, reference 4) to the following:

$$R_{\perp} \approx \left[\frac{\sqrt{\epsilon_{rl}} \cos \theta - (\epsilon_{r2} - \epsilon_{rl} \sin^2 \theta)^{1/2}}{\sqrt{\epsilon_{rl}} \cos \theta + (\epsilon_{r2} - \epsilon_{rl} \sin^2 \theta)^{1/2}} \right]^2 \quad (8)$$

$$R_{||} \approx \left[\frac{\epsilon_{r2} \cos \theta - \sqrt{\epsilon_{rl}} (\epsilon_{r2} - \epsilon_{rl} \sin^2 \theta)^{1/2}}{\epsilon_{r2} \cos \theta + \sqrt{\epsilon_{rl}} (\epsilon_{r2} - \epsilon_{rl} \sin^2 \theta)^{1/2}} \right]^2 \quad (9)$$

where subscripts 1 and 2 on ϵ_r refer to media 1 and 2 in a layered system and

R_{\perp} = power reflection coefficient for perpendicular polarization

$R_{||}$ = power reflection coefficient for parallel polarization

θ = angle of incidence, deg

51. The reflection coefficients versus incidence angle calculated from equations 8 and 9 for fresh water ($\epsilon_{r2} = 81$) and dry soil ($\epsilon_{r2} = 6$) with medium 1 being air ($\epsilon_{rl} = 1$) are shown in fig. 8. As has been stated (paragraph 45), at frequencies greater than a few megahertz, these media act as dielectrics (low-loss media) insofar as their reflecting properties are concerned. The transmitted wave is, however, rapidly attenuated by the effects of conductivity (i.e. in the factor α).

When $\theta = 0$

$$R = R_{\perp} = R_{||} = \left(\frac{\sqrt{\epsilon_{r2}} - \sqrt{\epsilon_{rl}}}{\sqrt{\epsilon_{r2}} + \sqrt{\epsilon_{rl}}} \right)^2 \quad (10)$$

and when medium 1 is air ($\epsilon_{rl} = 1$)

$$R = \left(\frac{\sqrt{\epsilon_{r2}} - 1}{\sqrt{\epsilon_{r2}} + 1} \right)^2 \quad \text{or} \quad \epsilon_{r2} = \left(\frac{1 + \sqrt{R}}{1 - \sqrt{R}} \right)^2 \quad (11)$$

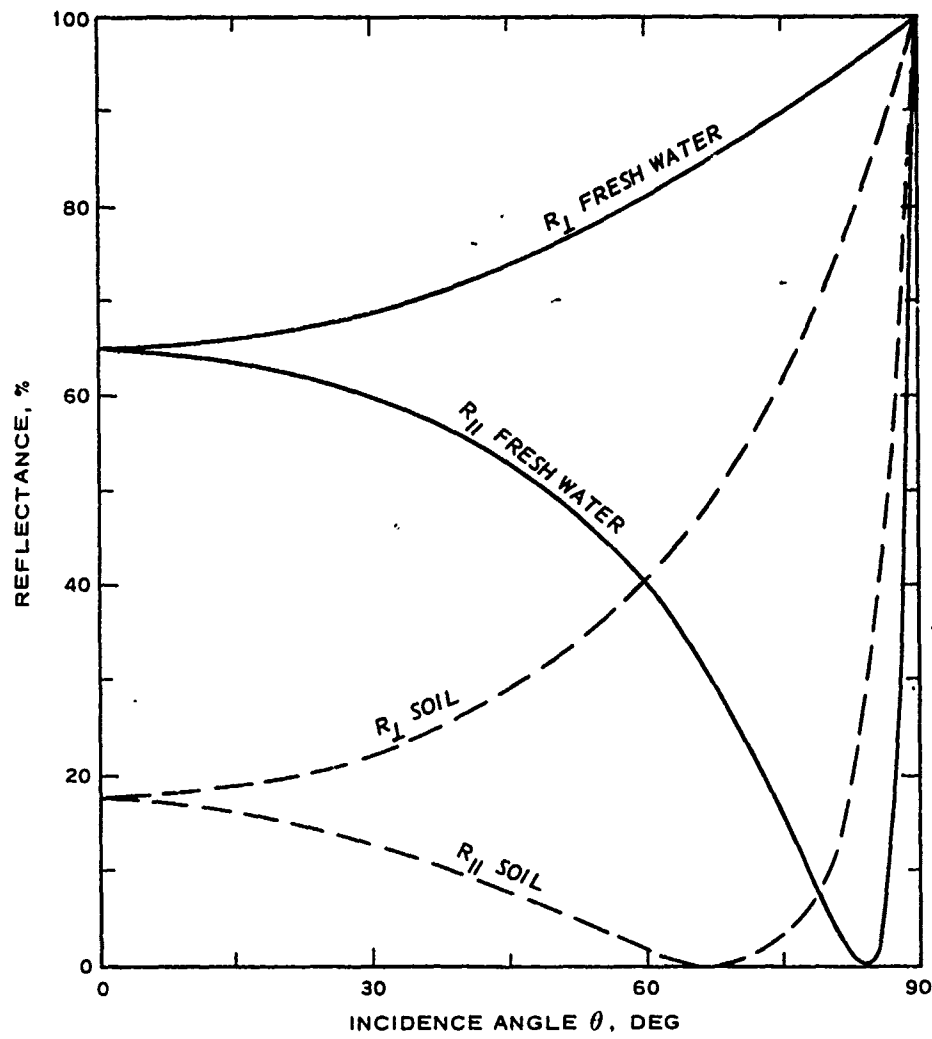


Fig. 8. Reflection coefficients of plane radio waves from soil and freshwater surfaces at frequencies greater than 10^6 Hz

52. Note that the reflectance in fig. 8 does not change significantly with incidence angle until θ reaches 10 or 15 deg; therefore, the slight increase in incidence angle caused by the separation of the transmitting and receiving antennas caused only minor changes in the measured reflectance values.

53. For a layered medium, subsurface reflections can combine with surface reflection and give widely varying results, depending on the thicknesses of the layers, the layers' electrical properties, and the wavelength of the transmitted signal. Consider the case of plane waves

at normal incidence to a target consisting of three media with three propagation factors (fig. 9).

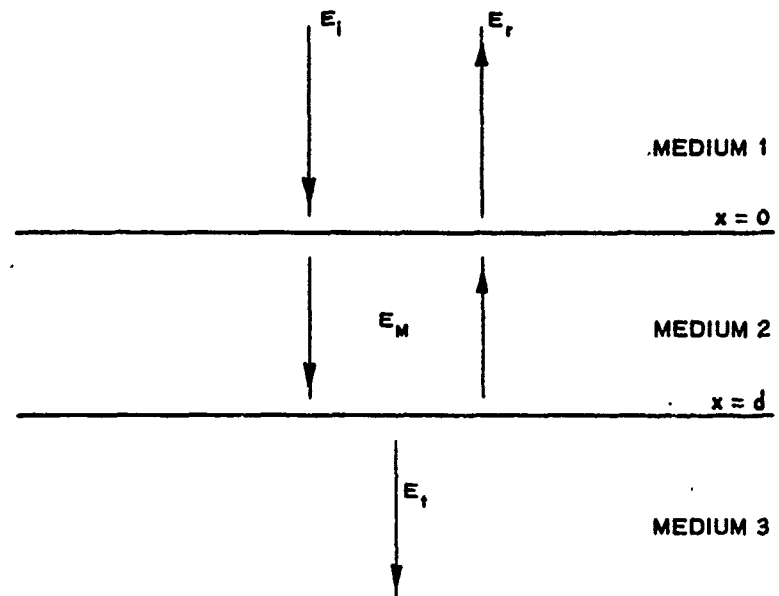


Fig. 9. Reflection and transmission of plane waves by a plane sheet at normal incidence

54. The electrical wave reflectance r_o in medium 1 can be written as⁵

$$\frac{E_r}{E_i} = r_o = \frac{r_{12} + r_{23} e^{-2\gamma_2 d}}{1 + r_{12} r_{23} e^{-2\gamma_2 d}} \quad (12)$$

where E_r and E_i are reflected and incident electric field intensity, respectively; r_{12} and r_{23} are electric wave reflections at the boundaries between media 1 and 2, and 2 and 3, respectively, as computed from

$$r_{12} = \frac{Z_2 - Z_1}{Z_2 + Z_1} \quad (13)$$

$$r_{23} = \frac{Z_3 - Z_2}{Z_3 + Z_2} \quad (14)$$

and d is layer thickness. Impedances Z are computed for each layer as

$$Z = \frac{j\omega\mu_0}{\gamma} \quad (15)$$

55. When equation 12 is multiplied by its complex conjugate, it becomes an equation for power reflectance.

$$R = |r_o|^2 = \frac{R_{12} + R_{23} e^{-4\alpha_2 d} + 2\sqrt{R_{12}R_{23}} e^{-2\alpha_2 d} \cos(2\beta_2 d + \theta_{12} - \theta_{23})}{1 + R_{12}R_{23} e^{-4\alpha_2 d} + 2\sqrt{R_{12}R_{23}} e^{-2\alpha_2 d} \cos(2\beta_2 d - \theta_{12} - \theta_{23})} \quad (16)$$

where

$R_{12} = |r_{12}|^2$ = power reflection coefficient at boundary between media 1 and 2

$R_{23} = |r_{23}|^2$ = power reflection coefficient at boundary between media 2 and 3

and θ_{12} and θ_{23} are defined by

$$r_{12} = |r_{12}| e^{j\theta_{12}}$$

$$r_{23} = |r_{23}| e^{j\theta_{23}}$$

56. As shown in a plot of equation 16 versus layer thickness measured in wavelengths (fig. 10), the power reflectance can have a number

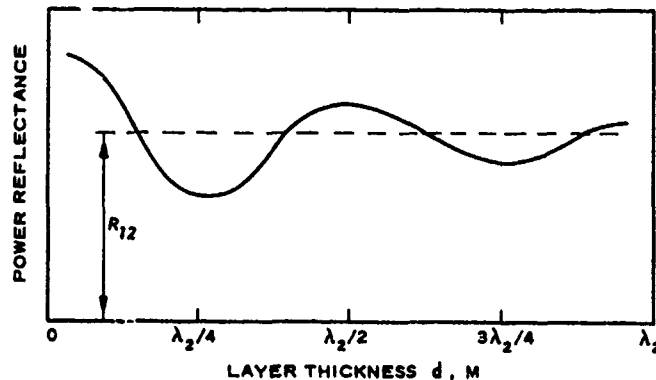


Fig. 10. Power reflectance at normal incidence as a function of layer thickness

of values at one single frequency, depending on the layer thickness d .

57. The power reflectance also varies with frequency when the layer thickness remains constant (fig. 11a). The positions of the maxima and minima of equation 16 for low-loss materials can be found by differentiating the reflectance expression with respect to frequency and by setting the results equal to zero (the value for slope at a maximum or minimum). The following results are thus obtained:

$$\frac{dR}{df} = 0 = K \left[\sin(2\beta_2 d - \theta_{23}) \cos \theta_{12} (1 - R_{12}) \left(1 - R_{23} e^{-4\alpha_2 d} \right) \right. \\ + \cos(2\beta_2 d - \theta_{23}) \sin \theta_{12} (1 + R_{12}) \left(1 + R_{23} e^{-4\alpha_2 d} \right) \\ \left. + 2\sqrt{R_{12} R_{23}} e^{-2\alpha_2 d} \sin 2\theta_{12} \right] \quad (17)$$

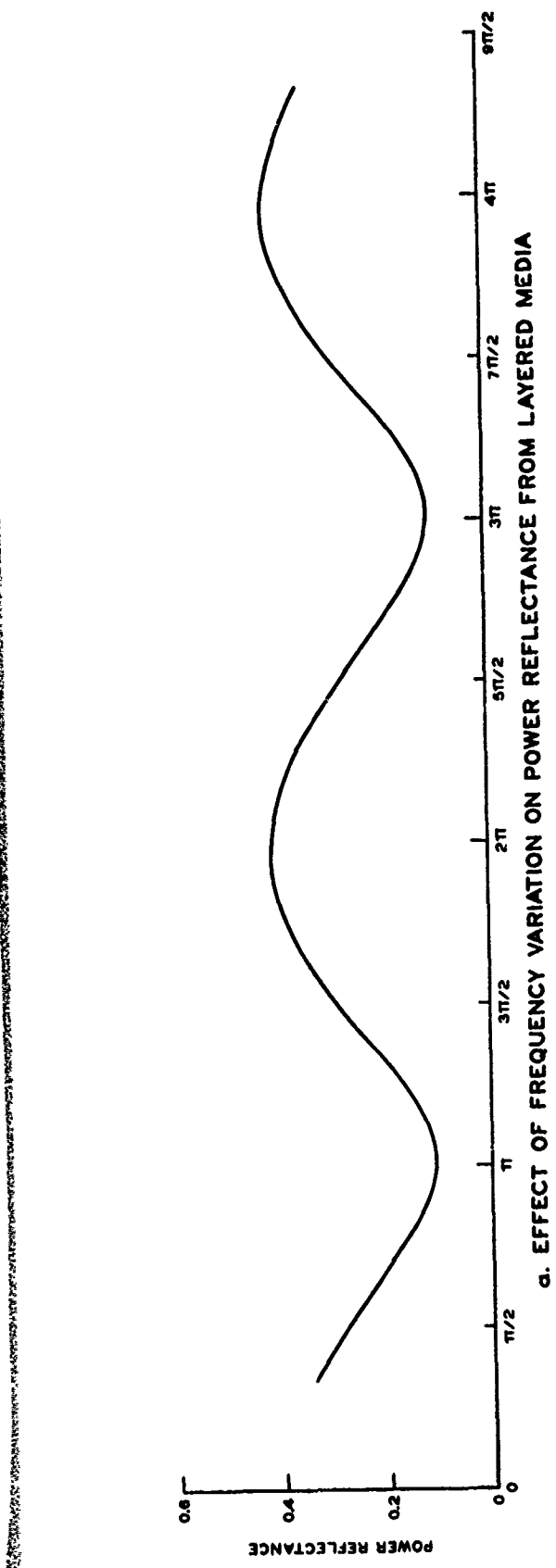
where

$$K = \frac{-8\pi d \left(\sqrt{\frac{\epsilon r_2}{c}} \right) \sqrt{R_{12} R_{23}} e^{-2\alpha_2 d}}{\left[1 + R_{12} R_{23} e^{-4\alpha_2 d} + 2\sqrt{R_{12} R_{23}} e^{-2\alpha_2 d} \cos(2\beta_2 d - \theta_{12} - \theta_{23}) \right]^2}$$

Thus, a maximum or minimum occurs for the power reflectance (equation 16) when

$$\sin(2\beta_2 d - \theta_{23}) \cos \theta_{12} (1 - R_{12}) \left(1 - R_{23} e^{-4\alpha_2 d} \right) \\ = -\cos(2\beta_2 d - \theta_{23}) \sin \theta_{12} (1 + R_{12}) \left(1 + R_{23} e^{-4\alpha_2 d} \right) \\ - 2\sqrt{R_{12} R_{23}} e^{-2\alpha_2 d} \sin 2\theta_{12} \quad (18)$$

This expression is shown graphically in fig. 11b where solution points occur at the intersections of the two curves. Although the distance from maximum to minimum (see fig. 11) is different from the distance from minimum to maximum, the period T_f (the distance between either adjacent maxima or minima) is single-valued and is displayed when $2\beta d$ increases by 2π . From the results of equation 7



$$\text{CURVE A: } A = \sin(2B_2d - \theta_{23}) \cos \theta_{12} (1 - R_{12}) (1 - R_{23} e^{-4\alpha_2 d})$$

$$\text{CURVE B: } B = - \left[\cos(2B_2d - \theta_{23}) \sin \theta_{12} (1 + R_{12}) (1 + R_{23} e^{-4\alpha_2 d}) + 2\sqrt{R_{12} R_{23}} e^{-2\alpha_2 d} \sin 2\theta_{12} \right]$$

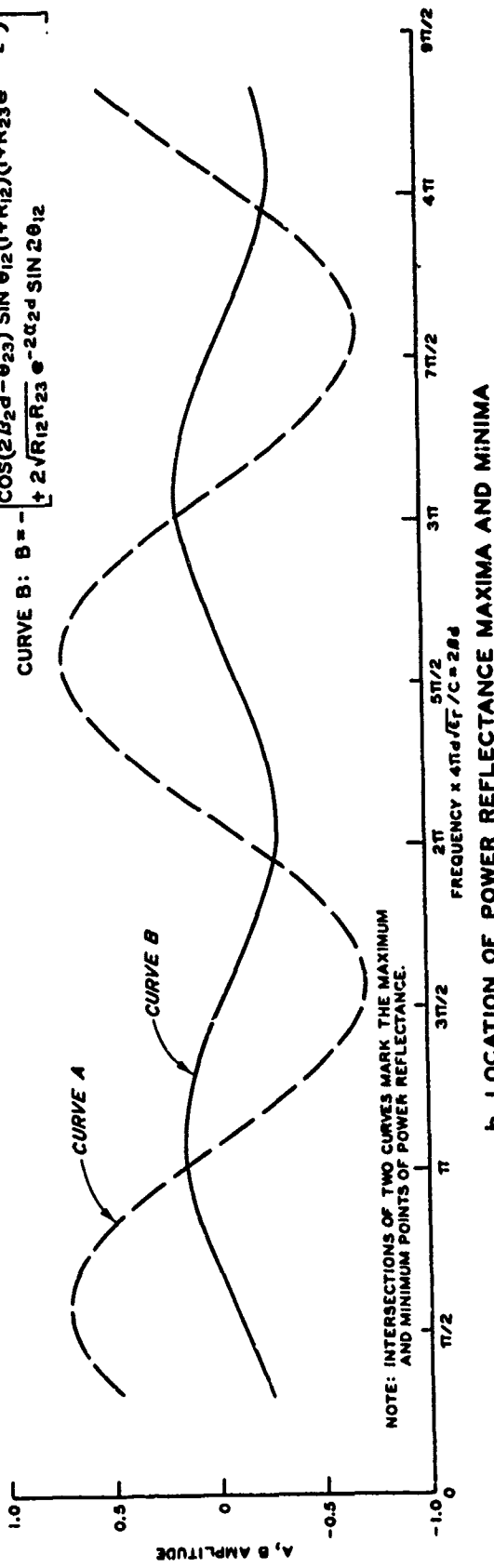


Fig. 11. Power reflectance and amplitude versus frequency

$$\frac{4\pi d(T_f)}{c} \sqrt{\epsilon_r} = 2\pi$$

and

$$d = \frac{c}{2\sqrt{\epsilon_r}} T_f \quad (19)$$

58. From equation 19, the layer thickness d can be obtained from the cyclic period T_f and the wave velocity $c/\sqrt{\epsilon_r}$ of that layer. Layer thickness can be estimated even when the minima and maxima are shifted slightly from their proper frequency positions because only the period of oscillation is required. Position shifts can be caused by rough surfaces, transition zones between materials, nonhomogeneous materials, effects of conductivity, and frequency dependence of the material's electrical properties. The accuracy of T_f is affected by the same things causing position shifts. However, wave interference phenomena degrade under these conditions, and before a significant reduction in T_f is observed, the cyclic pattern is no longer identifiable.

59. The results of equation 19 can be easily extended to multiple-layer sites where reflection from each interface causes characteristic periodic oscillations to appear in the total return. These periodic oscillations can be extracted by means of a correlation process. Repeated application of equation 19 can be used to determine these layer thicknesses when optical depth is used to replace the physical depth. The optical depth can be defined as the product of the physical depth and the square root of the relative dielectric constant. Calculations of these types were employed in the discussion presented in paragraphs 63-70. If the surface and subsurface components are to be separated from the total return, equation 16 must be carried one step further. An approximate expression for the maxima of equation 16 can be found by setting $\cos 2\beta d = 1$ (see fig. 11) as shown below.

$$R_{\max} = \left(\frac{\sqrt{R_{12}} + \sqrt{R_{23}} e^{-2\alpha_2 d}}{1 + \sqrt{R_{12} R_{23}} e^{-2\alpha_2 d}} \right)^2 \quad (20)$$

The approximate expression for the minima of equation 16 is found in a similar manner by setting $\cos 2\beta d = -1$:

$$R_{\min} = \left(\frac{\sqrt{R_{12}} - \sqrt{R_{23}} e^{-2\alpha_2 d}}{1 - \sqrt{R_{12} R_{23}} e^{-2\alpha_2 d}} \right)^2 \quad (21)$$

Then,

$$\sqrt{R_{23}} e^{-2\alpha_2 d} = \frac{1 - \sqrt{R_{\max} R_{\min}} \pm \sqrt{(R_{\max} - 1)(R_{\min} - 1)}}{\sqrt{R_{\max}} - \sqrt{R_{\min}}} \quad (22)$$

and

$$\sqrt{R_{12}} = \frac{R_{\max} + R_{\min}}{2 - (\sqrt{R_{\max}} - \sqrt{R_{\min}}) \sqrt{R_{23}} e^{-2\alpha_2 d}} \quad (23)$$

or

$$R_{12} = \left[\frac{\sqrt{R_{\max}} + \sqrt{R_{\min}}}{2 - (\sqrt{R_{\max}} - \sqrt{R_{\min}}) \sqrt{R_{23}} e^{-2\alpha_2 d}} \right]^2 \quad (24)$$

Note that if the subsurface component $\sqrt{R_{23}} e^{-2\alpha_2 d}$ is missing or negligible, $R_{\max} = R_{\min} = R$, and the surface component is $R = R_{12}$.

Discussion of Results

Surface reflectance

60. The level of the power reflectance curve is established by the surface reflectance from a homogeneous target material, or by the largest signal component from a layered site. If the surface reflectance has a larger amplitude than any of the subsurface components, the total subsurface reflectance will cycle around the surface reflectance. If a subsurface component has the largest amplitude, the surface reflectance will cycle around the subsurface component reflectance.

61. For the sites measured for this report, the surface reflectance was much larger than any of the subsurface components and was

assumed to be the average power reflectance over the range of 0.5 to 2.0 GHz (an approximation based on equation 24). This value was then substituted into equation 10 to calculate the relative dielectric constant of the surface. The results of these calculations are shown in table 2. The relative dielectric constants varied from 2.89 to 3.38 for the nine tests and averaged 3.12. This compares very well with the average value of 3.53 for the relative dielectric constant from L-band interferometer measurements (see paragraph 29). Note that the highway surface sloped away from the traffic center line (see fig. 3). The sloping surface of the test site would have the same effect as would operating at incidence angles other than 0 deg (see fig. 8). This effect was ignored in the analysis of data but could be reduced by operating with an antenna with a smaller beam width or by operating at a lower antenna height so that the illuminated area on the pavement surface was at the level point between the two traffic lanes.

62. The antenna height, however, cannot be reduced indefinitely. For a given antenna operating at a given frequency, a point will be reached, as the height is reduced, where the power density on the target area is not uniform or easily predictable (i.e. the near field of the antenna). Although some of the data presented in this report were actually measured in the near field of the antenna, accuracy was not sacrificed, since the reflectance of the test site was referenced to the standard reflectance, with both at the same range (see paragraph 35). Also, since the layer thicknesses were small compared with the antenna range (or height), plane wave analysis could still be used.

Subsurface reflectances

63. Cyclic patterns are present in all the power reflectance curves (plates 1-9). Curves obtained from measurements at the same site have the same general appearance over the frequency range of 0.25 to 2.0 GHz and differ only slightly from site to site. The curves have high-frequency signal components (noise) riding on top of the low-frequency cyclic patterns. The noise does not appear to contain information about the test site and is probably the result of digitizing procedures and minor changes in transmitted power.

64. In order to extract layer thickness from the reflectance data, the period of the oscillations had to be determined. This was done by separating the original power reflectance curve into its various signal components. This procedure is illustrated in fig. 12, where two periodic waves of decreasing amplitudes and a noise component are extracted from the original power reflectance curve. The periods of the waves used in this reconstruction process can be used in equation 19 to compute layer thicknesses.

65. Another method used to extract the period of oscillation in addition to the graphical technique described above was the cross-correlation technique. The data were cross-correlated with a sine wave, and the correlation coefficient showed an increased amplitude when the sine wave period was the same as that of the periodic data. A fast Fourier transform (FFT) computer program with the following modifications was used to compute the correlations (see Appendix A):

- a. The average of the power reflectance data (384 points equally spaced over 0.5 to 2.0 GHz) was computed and subtracted from each data point.
- b. Data points with zero amplitude were added to raise the total number of input data points to 2048 (FFT program requires that the number of data points be a binary number such as 512, 1024, 2048, etc). The number 2048 was selected so that the cross-correlation plots would have a smooth continuous appearance when plotted by the computer. This gives an equivalent frequency range to the data record of 8.0 GHz.
- c. The amplitudes of the FFT coefficients were multiplied by 5.333 (the ratio of 2048 to 384) to correct for the effect of the added zero-amplitude points.
- d. The first five harmonics were not used (i.e. the first five harmonics had periods longer than the data record and, therefore, would not have computed properly).

66. The results of this correlation process are shown in plates 10-12, for which the optical depth was computed as follows:

$$\text{Optical depth in meters} = \frac{c}{2T_f} = 0.01875n \quad (25)$$

where n is the harmonic number from the FFT computation. Since there

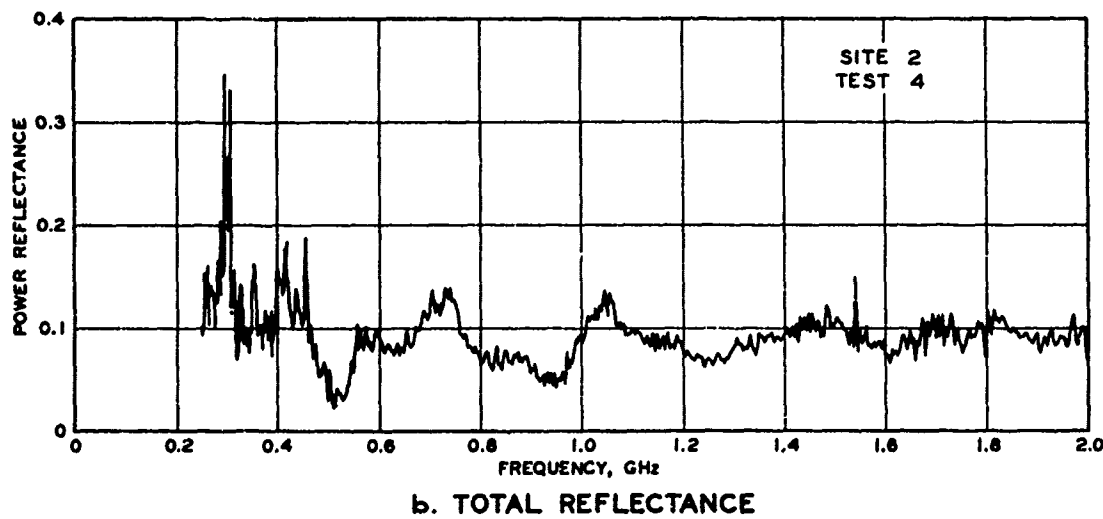
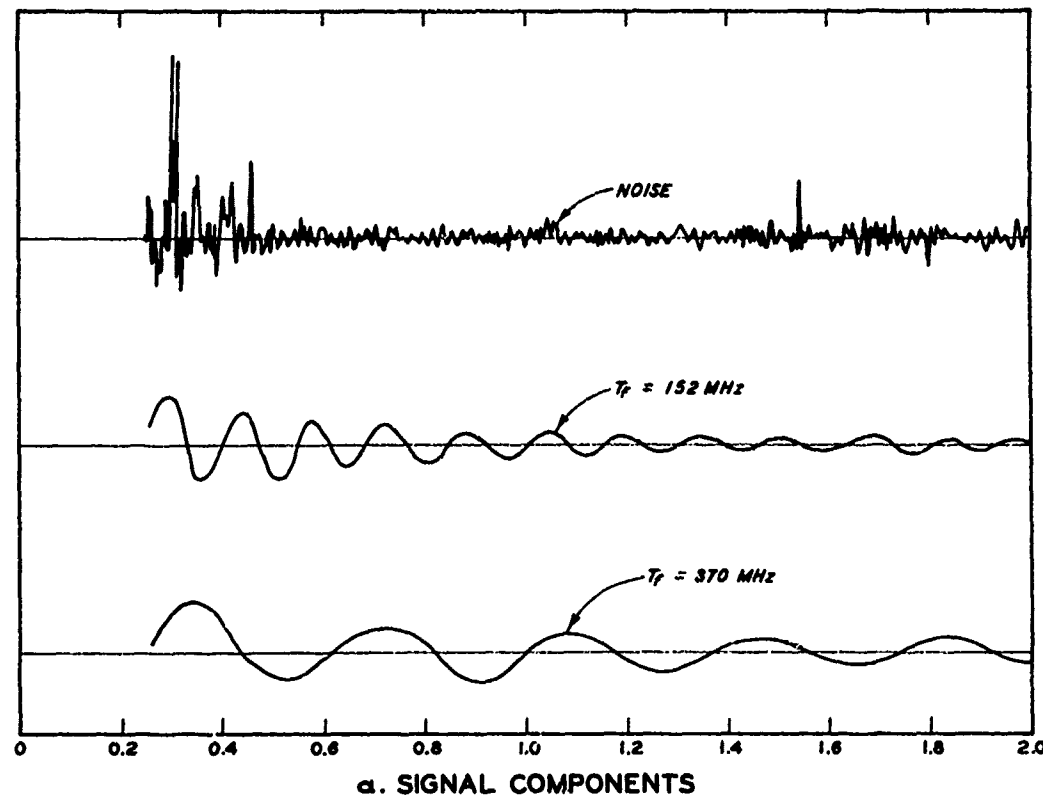


Fig. 12. Reconstructed power reflectance curve

were two layers (and, therefore, two transition zones) in the highway foundation, each plot of correlation coefficient versus optical depth showed two peaks. The first peak, at approximately 0.4 m, was easily identified in each plate and indicated the optical depth to the bottom of the asphaltic concrete layer (table 2). The second main peak indicated the optical depth to the second interface (i.e. between the clay-gravel base material and the silt foundation). This peak was easily identified as the second largest peak in plate 10 for site 1. The second peak for site 2 (plate 11) was also taken as the second largest peak, although there appeared to be a double peak associated with this interface. The second peak for site 3 (plate 12) was somewhat more difficult to pick out with only a single measurement being used; however, the location for the second peak was found based on shape similarity when all three curves were compared.

67. The remaining peaks present in plate 10 were probably caused by the analysis process itself; short data records can produce small peaks in the correlation curve at certain frequencies, depending on the character of the data. Long data records without sine wave distortion reduce the amplitudes of the small, ambiguous correlation peaks.

68. The averages of the correlation curves from each site over the optical depth range of 0-2 m are shown in fig. 13. The amplitudes of the small, ambiguous correlation peaks were reduced from those of the individual curves, since they were displaced from curve to curve. The peaks that were due to interface reflectances were maintained, since they were found at nearly the same optical depth in each measurement. The layer thicknesses were calculated by use of the following procedures:

- a. Determine the optical thickness of the asphaltic concrete layer (i.e. the optical depth location of the maximum of the first peak).
- b. Calculate the asphaltic concrete thickness by dividing the optical thickness by the square root of the asphaltic concrete relative dielectric constant ($\epsilon_r = 3.53$).
- c. Determine the optical thickness of the clay-gravel base layer (i.e. the difference in optical depth location between the maxima of the first and second peaks).
- d. Calculate the clay-gravel thickness by dividing the

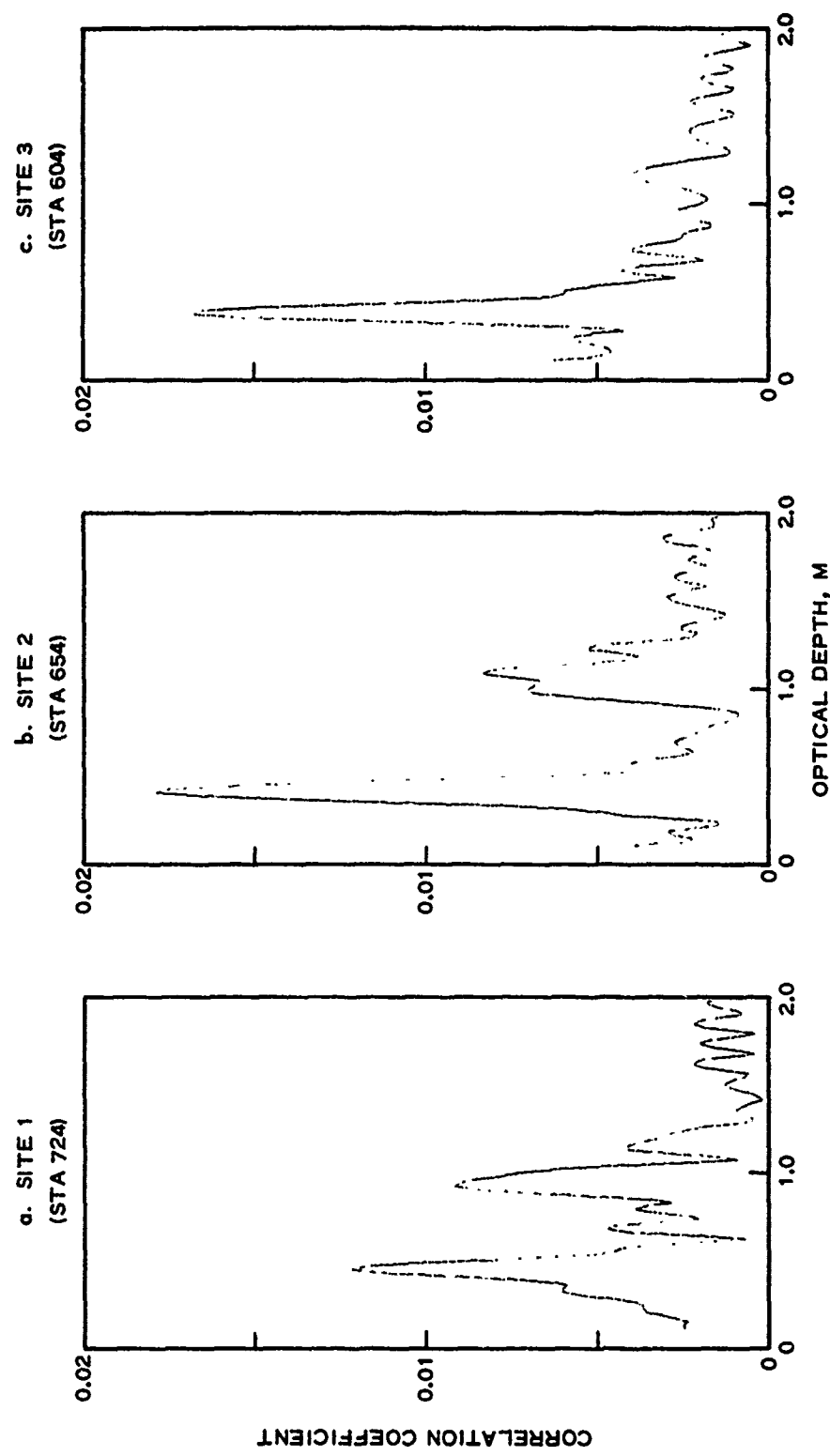


Fig. 13. Average optical thickness curves for sites 1, 2, and 3

optical thickness by the square root of the clay-gravel relative dielectric constant ($\epsilon_r = 6.5$).

69. The results of these procedures are tabulated below for the average data in fig. 13. The values for estimated thickness from ground measurements are taken from table 1.

Site No.	<u>Swept-Frequency Radar Measurements</u>		
	<u>Optical Thickness, m</u>	<u>Predicted Thickness, m</u>	<u>Thickness Estimated from Ground Measurements, m</u>
<u>Asphaltic Concrete</u>			
1	0.455	0.242	0.226
2	0.415	0.221	0.210
3	0.380	0.202	0.214
<u>Clay-Gravel Base</u>			
1	0.465	0.182	0.133 - 0.186
2	0.670	0.263	0.209 - 0.262
3	0.790	0.310	0.309 - 0.362

Note that for all three sites, the difference between the radar measurements and ground measurements for the asphaltic concrete layer was 1.6 cm or less (i.e. error of 7 percent or less). For the clay-gravel base, the radar measurement fell within the range of ground measurements for sites 1 and 3 and was outside the range of values for site 2 by only 1 mm.

70. If the same techniques were used to predict thickness of layers from each of the single reflectance tests (as listed in table 2), some decrease in the accuracy of the computed thicknesses would occur, as shown in the variation from test to test at each site. For example, predicted thicknesses of the asphaltic concrete varied from 0.239 to 0.242 m, 0.221 to 0.226 m, and 0.199 to 0.210 m for sites 1, 2, and 3, respectively. Predicted thicknesses of the clay-gravel base varied from 0.182 to 0.188 m, 0.220 to 0.276 m, and 0.288 to 0.329 m for sites 1, 2, and 3, respectively.

PART IV: CONCLUSIONS AND RECOMMENDATIONS

Conclusions

71. Based on the test results reported herein, the following conclusions are considered warranted:

- a. Swept-frequency radar measurements over the frequency range of 0.5 to 2.0 GHz can be used to estimate power reflectance from the surface material of highway pavement structures and to determine the amplitude of the subsurface contribution. These measurements make possible estimates of the electrical properties of each of the materials.
- b. Layered materials produce interference patterns in the power reflectance curves over the frequency range of 0.25 to 2.0 GHz. Interference patterns can be used to calculate both the optical thickness of each layer and, with an adjustment made for wave velocity in the material, the physical thickness of each layer.
- c. Insufficient data were obtained in this program to show whether the frequencies of 2.0 to 8.0 GHz are as effective as those of 0.25 to 2.0 GHz in determining layered material properties.

Recommendations

72. It is recommended that:

- a. Field tests be conducted on portland-cement concrete highways to determine the capability of the swept-frequency radar system to measure depths to reinforcing steel and layer thicknesses in the pavement structure.
- b. Additional tests be made at frequencies of 2.0 to 8.0 GHz to determine the effectiveness in measuring surface and subsurface material properties at these ranges. This would require the procurement of more efficient antennas to propagate the energy at these frequencies and the modification of the signal recording equipment to increase the accuracy of the data.
- c. The system be modified (both the system size and method of recording) so that continuous records can be made of layer thicknesses as a vehicle containing a swept-frequency radar system travels along the highway.

d. Comprehensive tests be initiated to determine the basic electrical properties of highway materials at various microwave frequencies and to establish correlations between these properties and material quality.

LITERATURE CITED

1. Davis, B. R., Lundien, J. R., and Williamson, A. N., Jr., "Feasibility Study of the Use of Radar to Detect Surface and Ground Water," Technical Report No. 3-727, Apr 1966, U. S. Army Engineer Waterways Experiment Station, CE, Vicksburg, Miss.
2. Lundien, J. R., "Terrain Analysis by Electromagnetic Means; Radar Responses to Laboratory Prepared Soil Samples," Technical Report No. 3-693, Report 2, Sep 1966, U. S. Army Engineer Waterways Experiment Station, CE, Vicksburg, Miss.
3. _____, "Terrain Analysis by Electromagnetic Means; Laboratory Measurements of Electromagnetic Propagation Constants in the 1.0- to 1.5-GHZ Microwave Spectral Region," Technical Report No. 3-693, Report 5, Feb 1971, U. S. Army Engineer Waterways Experiment Station, CE, Vicksburg, Miss.
4. Stratton, J. A., Electromagnetic Theory, 1st ed., McGraw-Hill, New York, 1941.
5. Von Hippel, A. R., Dielectrics and Waves, Wiley, New York, 1954.
6. Reference Data for Radio Engineers, 5th ed., Sams and Co., Indianapolis, Ind., 1968.
7. Blackman, R. B. and Tukey, J. W., The Measurement of Power Spectra, Dover, New York, 1958.

Table 1
Highway Data

	Site 1 (Sta 724)	Site 2 (Sta 654)	Site 3 (Sta 604)
Measured asphaltic concrete thickness in traffic lane X_0 , m	0.226	0.210	0.214
Measurements at center of test site:			
Asphaltic concrete thickness at edge of shoulder X_1 , m	0.146	0.124	0.102
Clay-gravel base thickness at edge of shoulder X_3 , m	0.286	0.359	0.483
Asphaltic concrete thickness at edge of emergency lane X_2 , m	0.121	0.098	0.083
Clay-gravel base thickness at edge of emergency lane X_4 , m	0.311	0.394	0.552
Measurements 1.83 m east of test site center:			
Asphaltic concrete thickness at edge of shoulder X_1 , m	0.121	0.121	0.114
Clay-gravel base thickness at edge of shoulder X_3 , m	0.305	0.375	0.470
Measurements 1.83 m west of test site center:			
Asphaltic concrete thickness at edge of shoulder X_1 , m	0.140	0.130	0.095
Clay-gravel base thickness at edge of shoulder X_3 , m	0.305	0.371	0.489
Maximum thickness of clay-gravel base in traffic lane X_5 , m	0.186	0.262	0.362
Minimum thickness of clay-gravel base in traffic lane X_6 , m	0.133	0.209	0.309
Moisture content measured during highway construction, %:			
Clay-gravel base*	4.4	4.5	4.8
Silt foundation	22.0	18.0	16.6
Dry density measured during highway construction, g/cm ³ :			
Clay-gravel base	2.04	1.94	2.19
Silt foundation	1.64	1.58	1.64

* Average moisture contents of clay-gravel base material, measured shortly after radar measurements were made, were 7.6%, 7.2%, and 6.8% for sites 1, 2, and 3, respectively. The moisture content samples were taken at the edge of the asphaltic concrete near the bottom of the clay-gravel base.

Table 2
 • Results From Highway Data Obtained with Swept-Frequency Radar
 (0.5 to 2.0 GHz)

	Site 1 (Sta. 724)			Site 2 (Sta. 654)			Site 3 (Sta. 604)			
	<u>Test 1</u>		<u>Test 2</u>	<u>Test 3</u>	<u>Test 4</u>		<u>Test 5</u>	<u>Test 6</u>	<u>Test 7</u>	
	<u>Test 8</u>	<u>Test 9</u>							<u>Test 8</u>	<u>Test 9</u>
Average power reflectance	0.0675	0.0722	0.0767	0.0871	0.0744	0.0822	0.0764	0.0673	0.0843	
Predicted asphaltic concrete relative dielectric constant	2.90	3.01	3.12	3.38	3.14	3.26	3.11	2.89	3.31	
Asphaltic concrete optical thickness, m	0.455	0.455	0.450	0.415	0.415	0.425	0.395	0.380	0.375	
Asphaltic concrete predicted thickness, * m	0.242	0.242	0.239	0.221	0.221	0.226	0.210	0.202	0.199	
Clay-gravel base optical thickness, m	0.480	0.465	0.465	0.560	0.705	0.640	0.735	0.790	0.840	
Clay-gravel base predicted thickness, ** m	0.188	0.182	0.182	0.220	0.276	0.251	0.288	0.310	0.329	

42

* Asphaltic concrete $\epsilon_r = 3.53$ (i.e. the average of relative dielectric constants from L-band interferometer measurements).
 ** Clay-gravel base $\epsilon_r = 6.5$.

POWER REFLECTANCE
VS
FREQUENCY
HIGHWAY 1 TESTS
SITE 1 (STA 724)
TEST 1

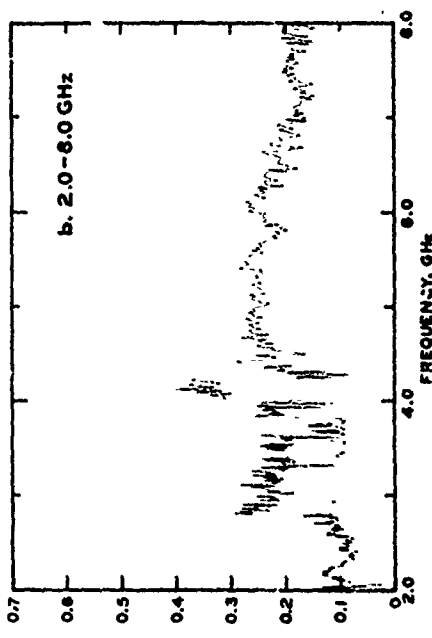
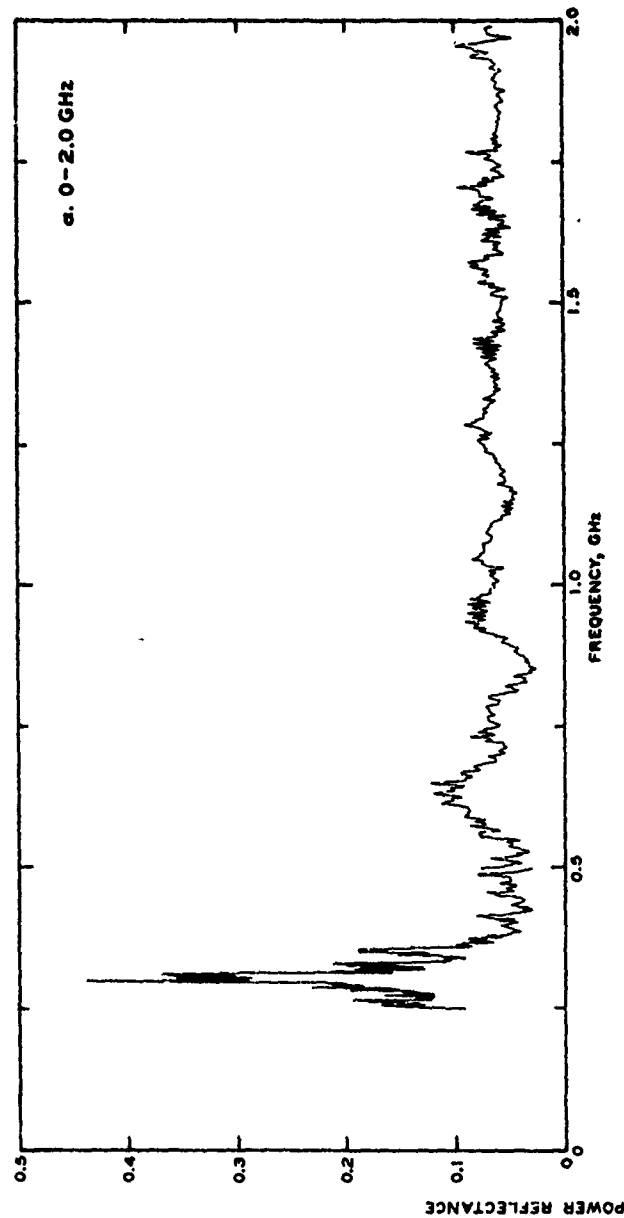


PLATE I

43

POWER REFLECTANCE
VS
FREQUENCY
HIGHWAY TESTS
SITE 1 (STA 724)
TEST 2

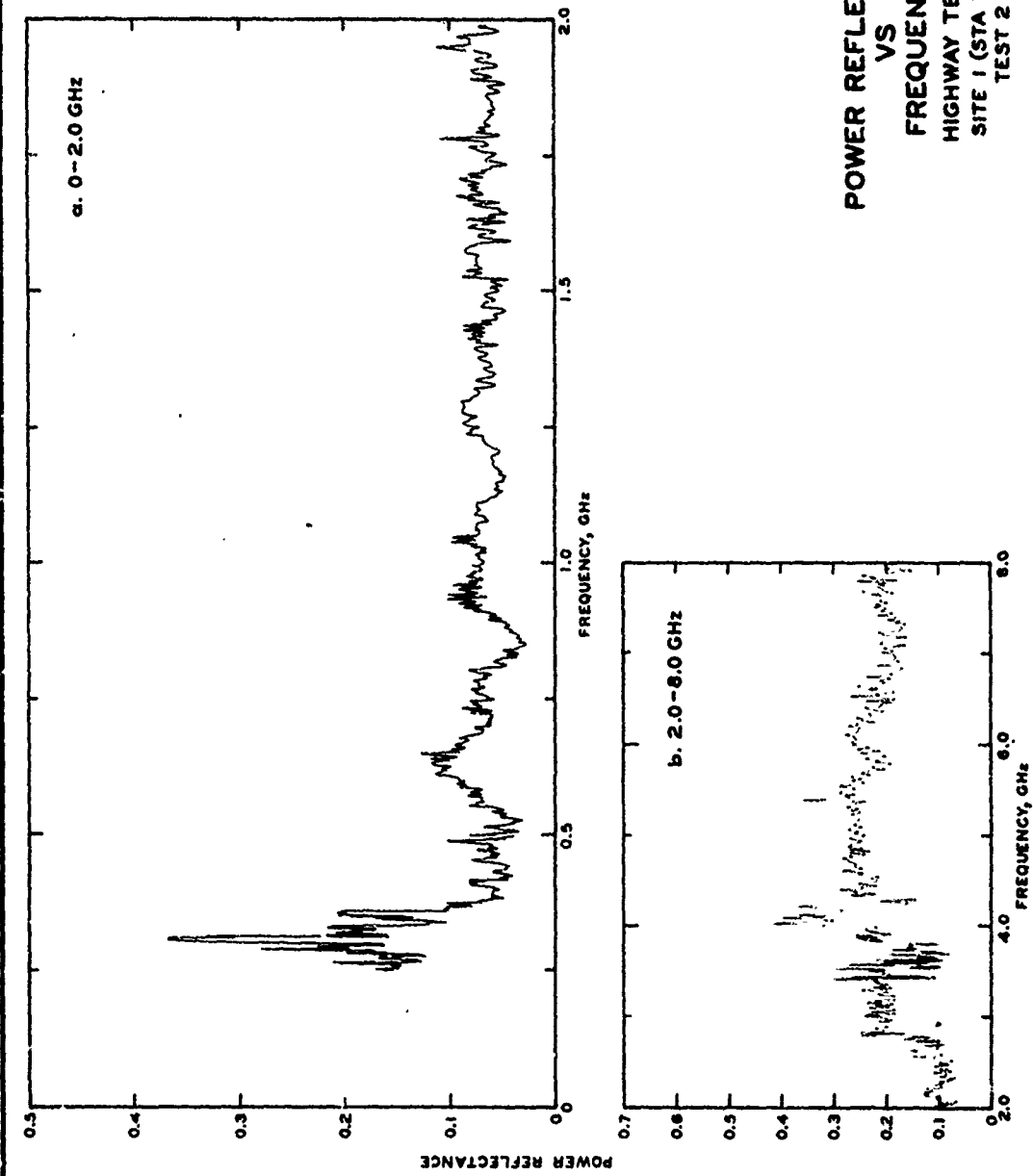


PLATE 2

44.

POWER REFLECTANCE
VS
FREQUENCY
HIGHWAY TESTS
SITE 1 (STA 724)
TEST 3

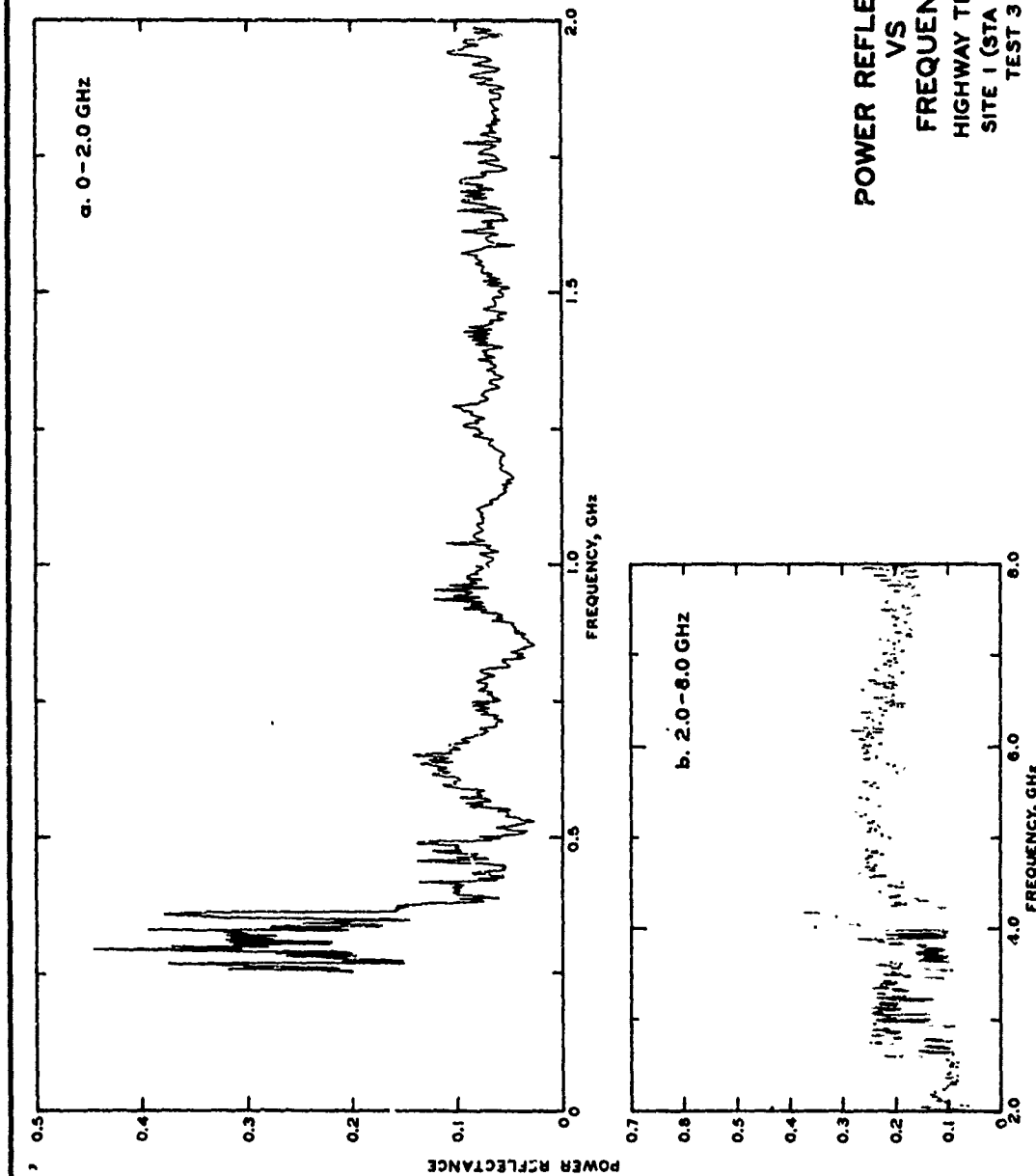


PLATE 3

45

POWER REFLECTANCE
VS
FREQUENCY
HIGHWAY TESTS
SITE 2 (STA 654)
TEST 4

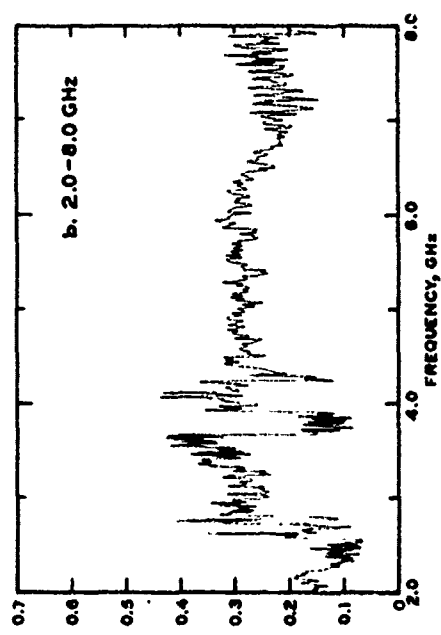
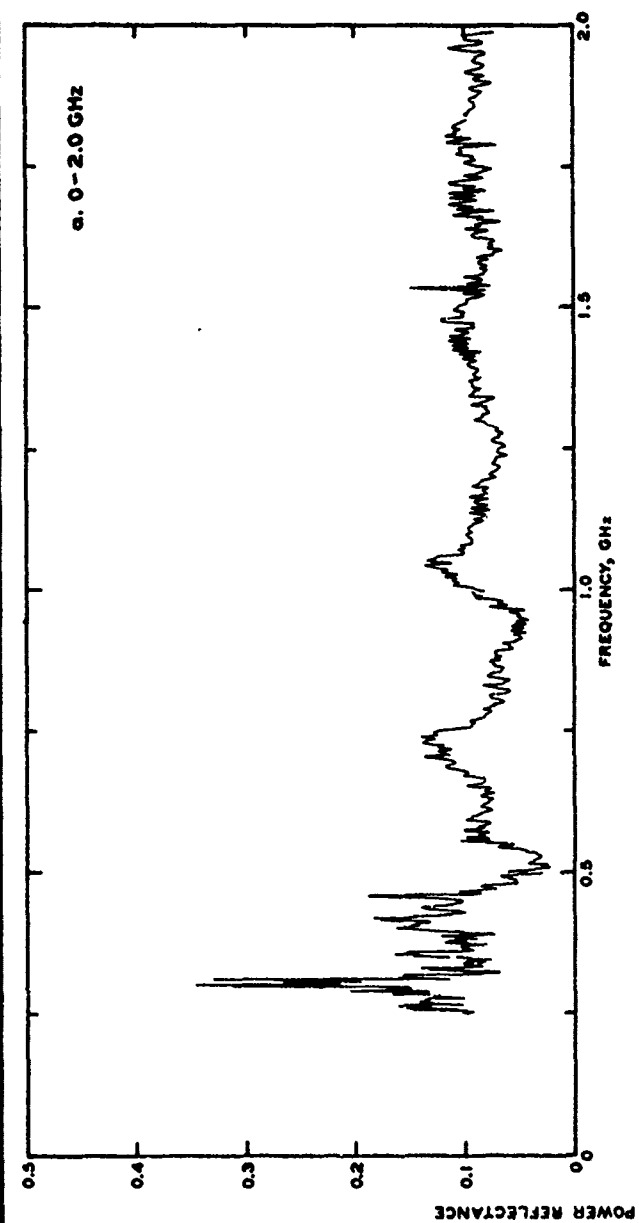


PLATE 4

46

POWER REFLECTANCE
VS
FREQUENCY
HIGHWAY TESTS
SITE 2 (STA 854)
TEST 5

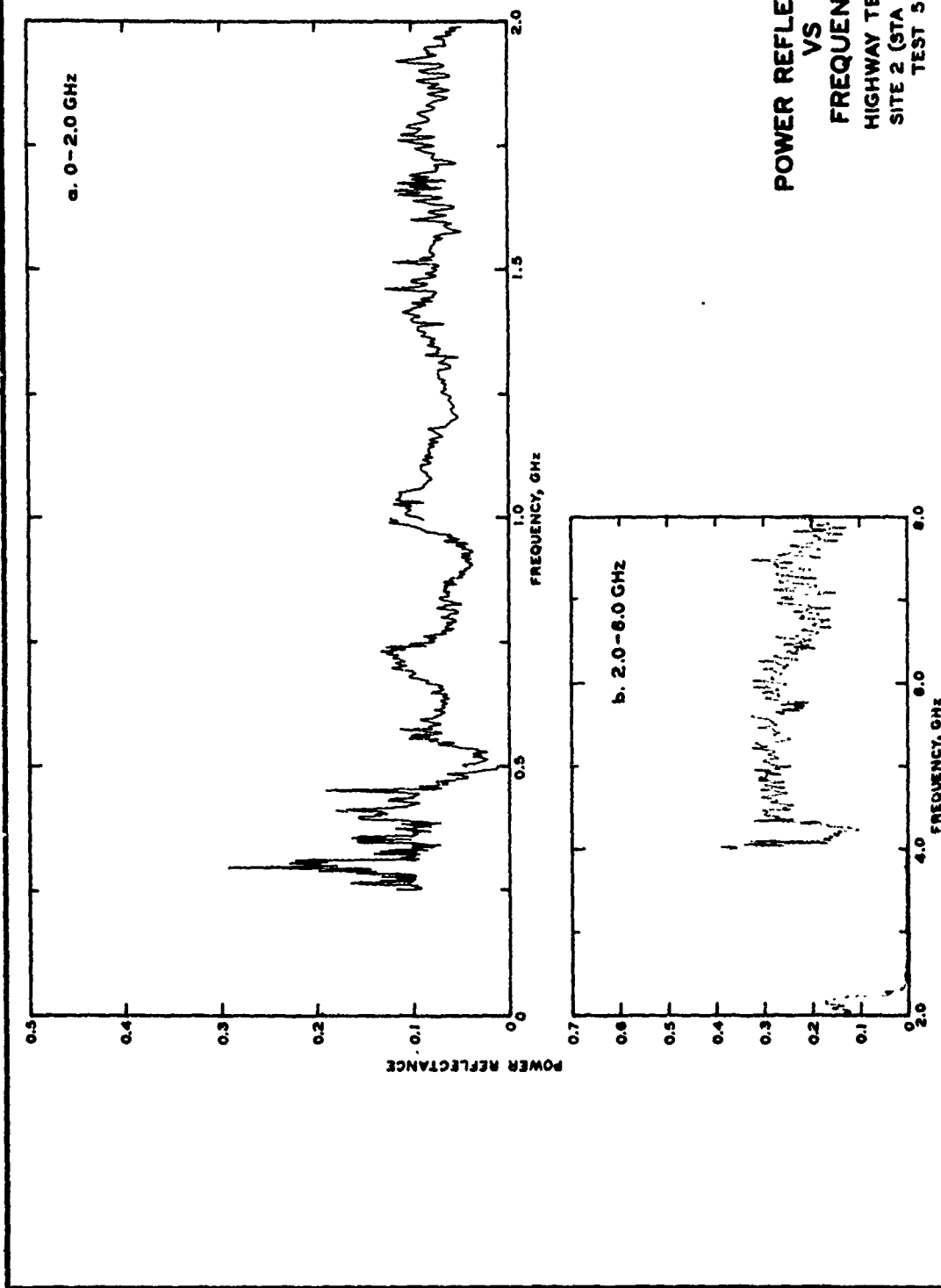


PLATE 5

POWER REFLECTANCE
VS
FREQUENCY
HIGHWAY TESTS
SITE 2 (STA 654)
TEST 6

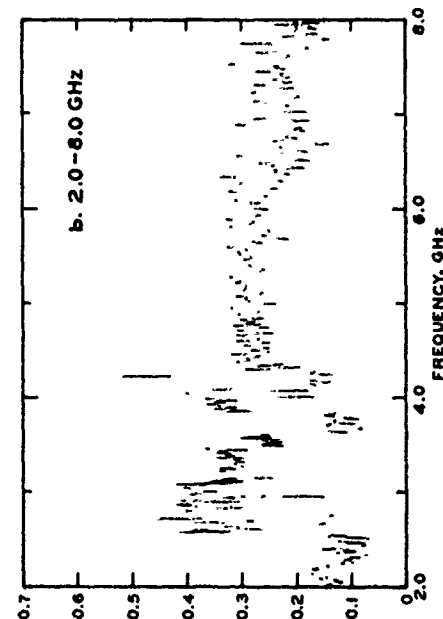
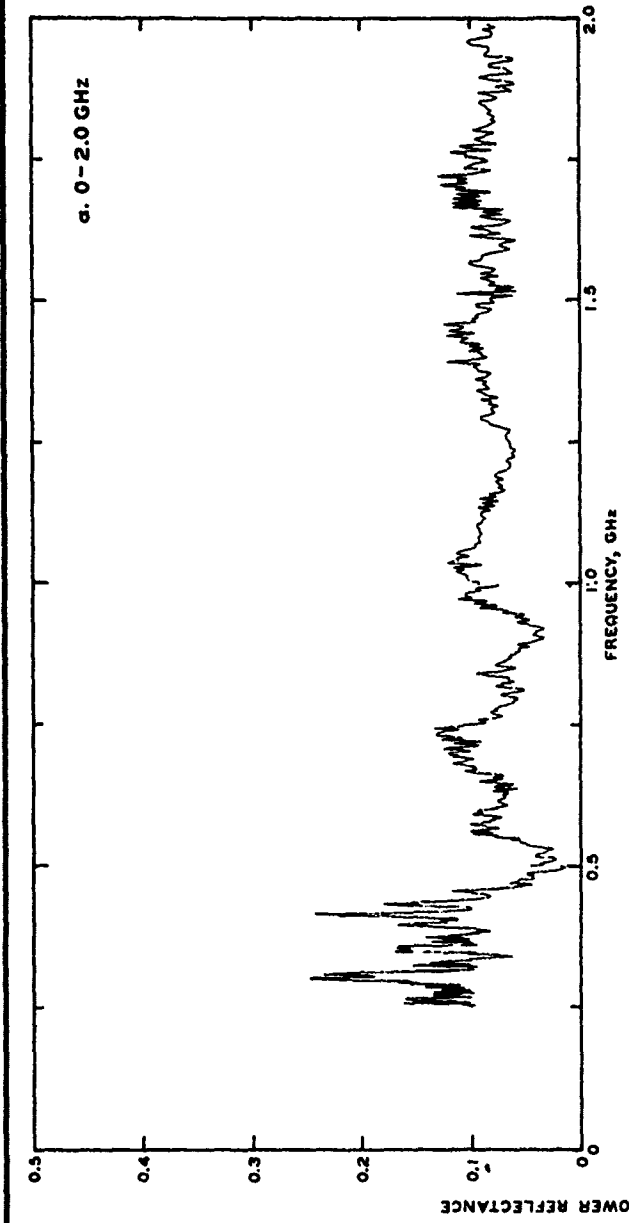
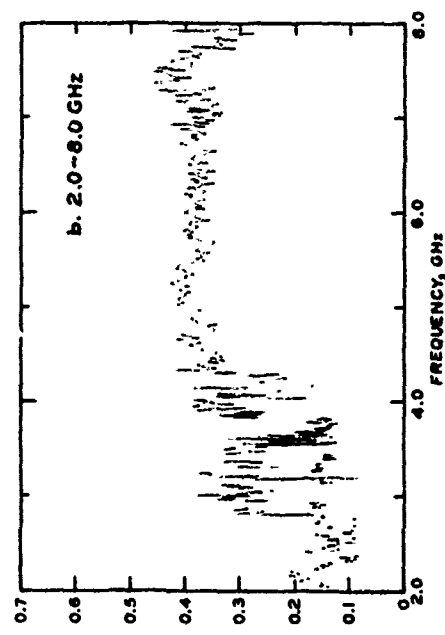
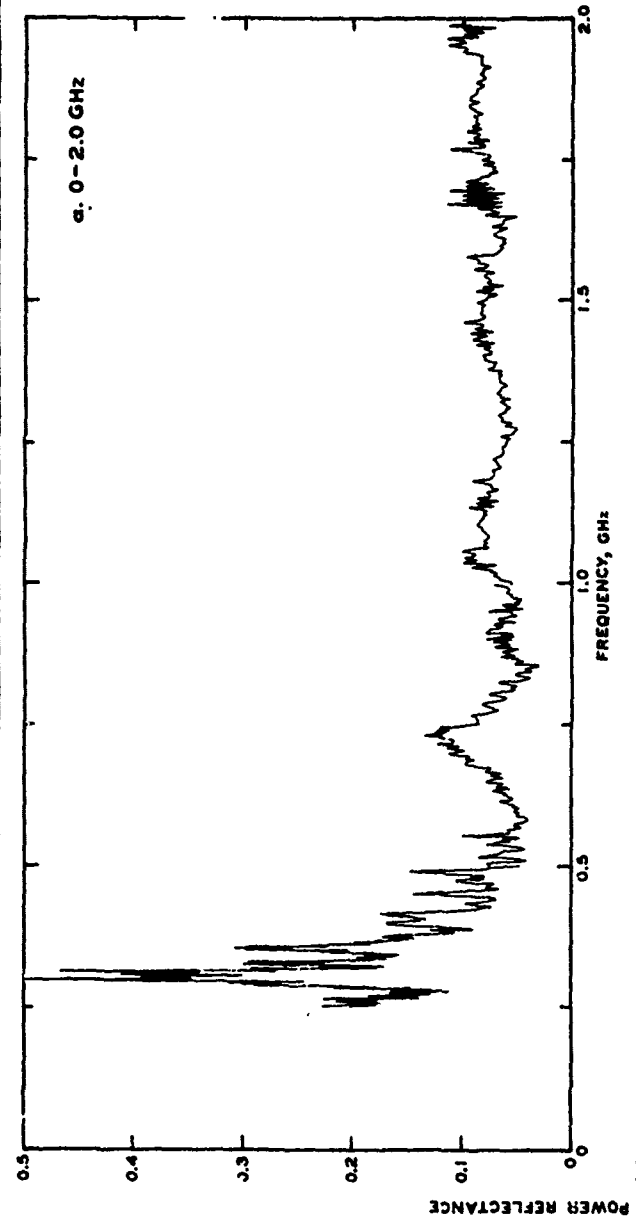


PLATE 6

48

POWER REFLECTANCE
VS
FREQUENCY
HIGHWAY TESTS
SITE 3 (STA 604)
TEST 7



POWER REFLECTANCE
VS
FREQUENCY
HIGHWAY TESTS
SITE 3 (STA 604)
TEST 8

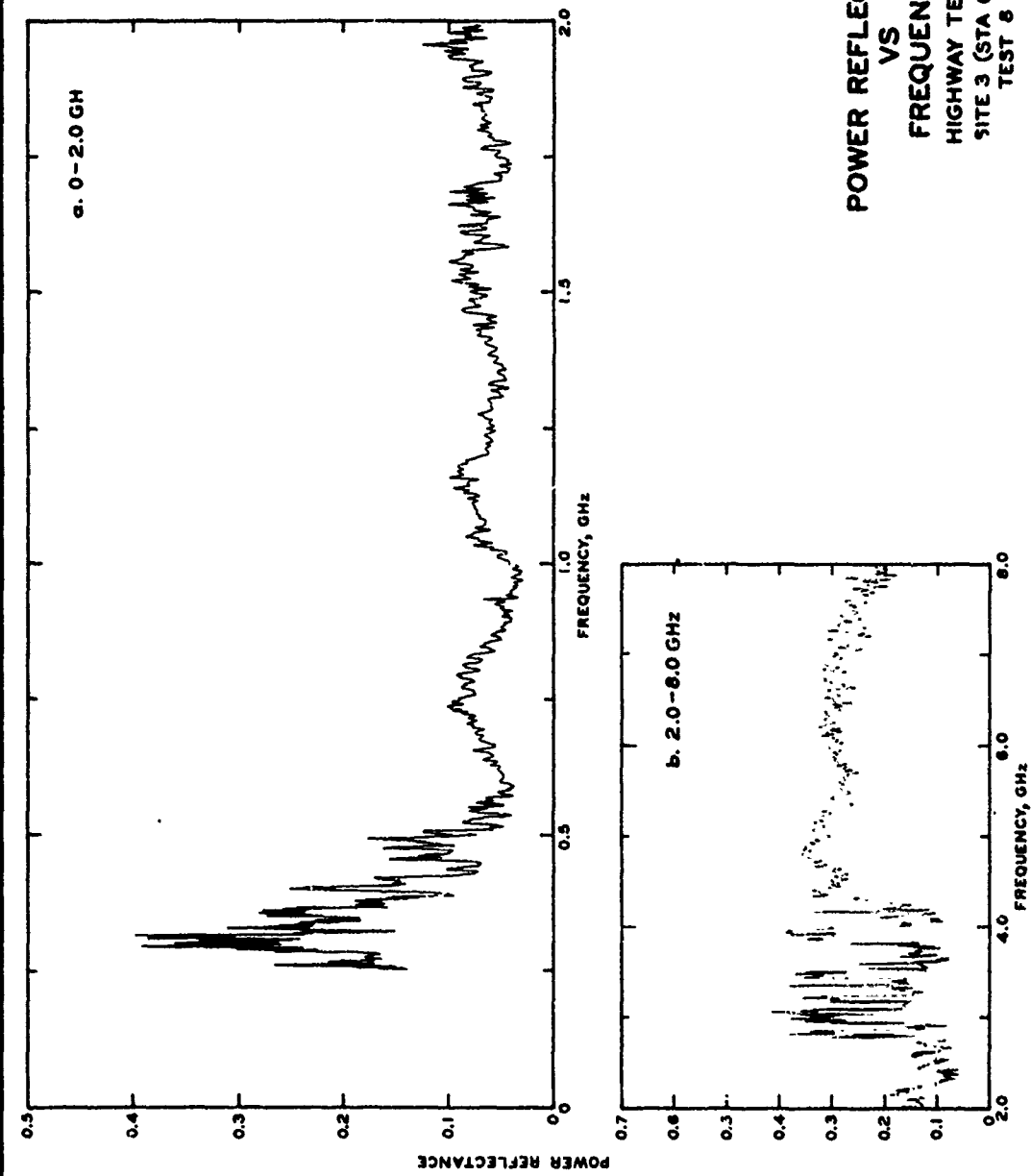
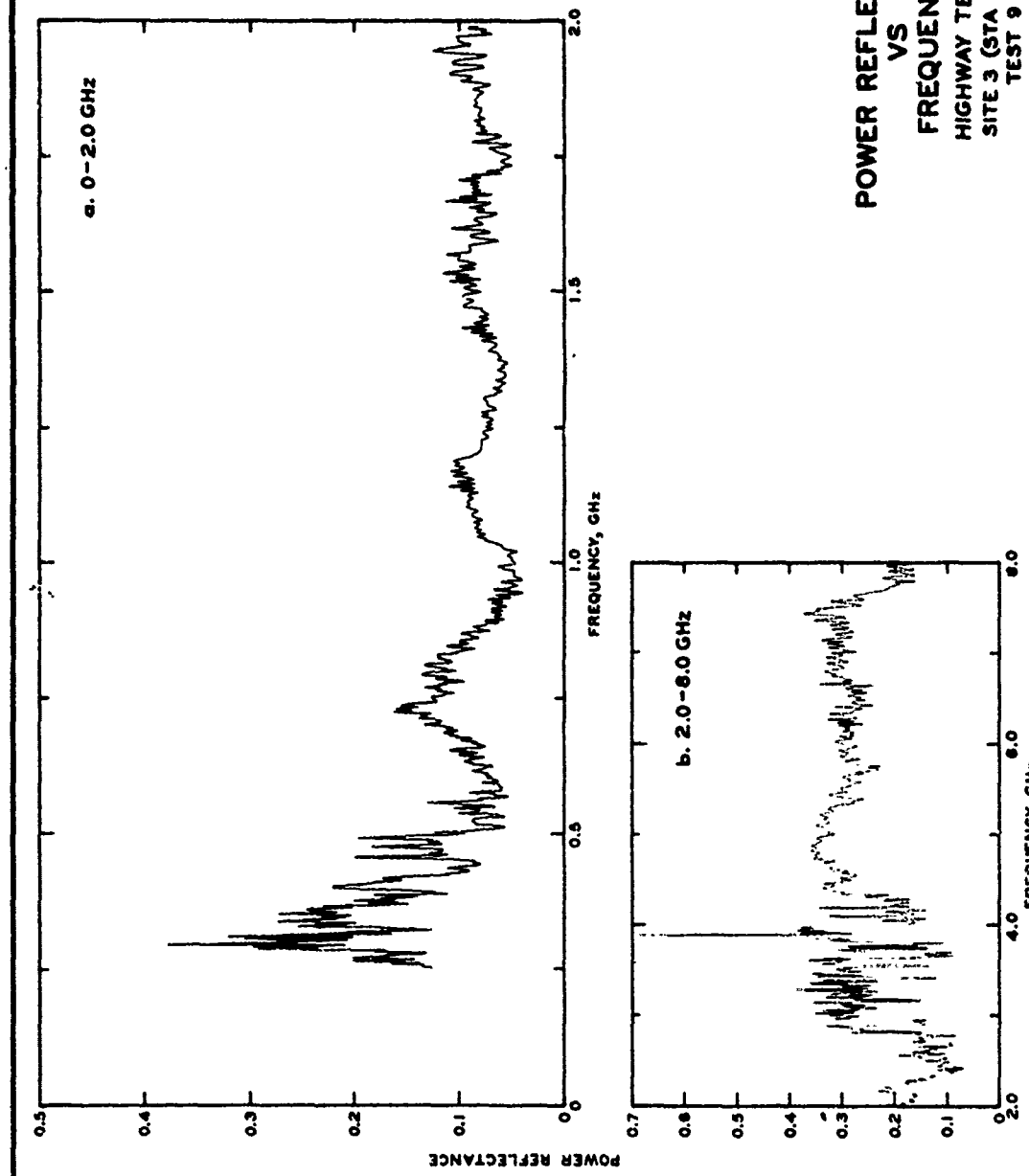
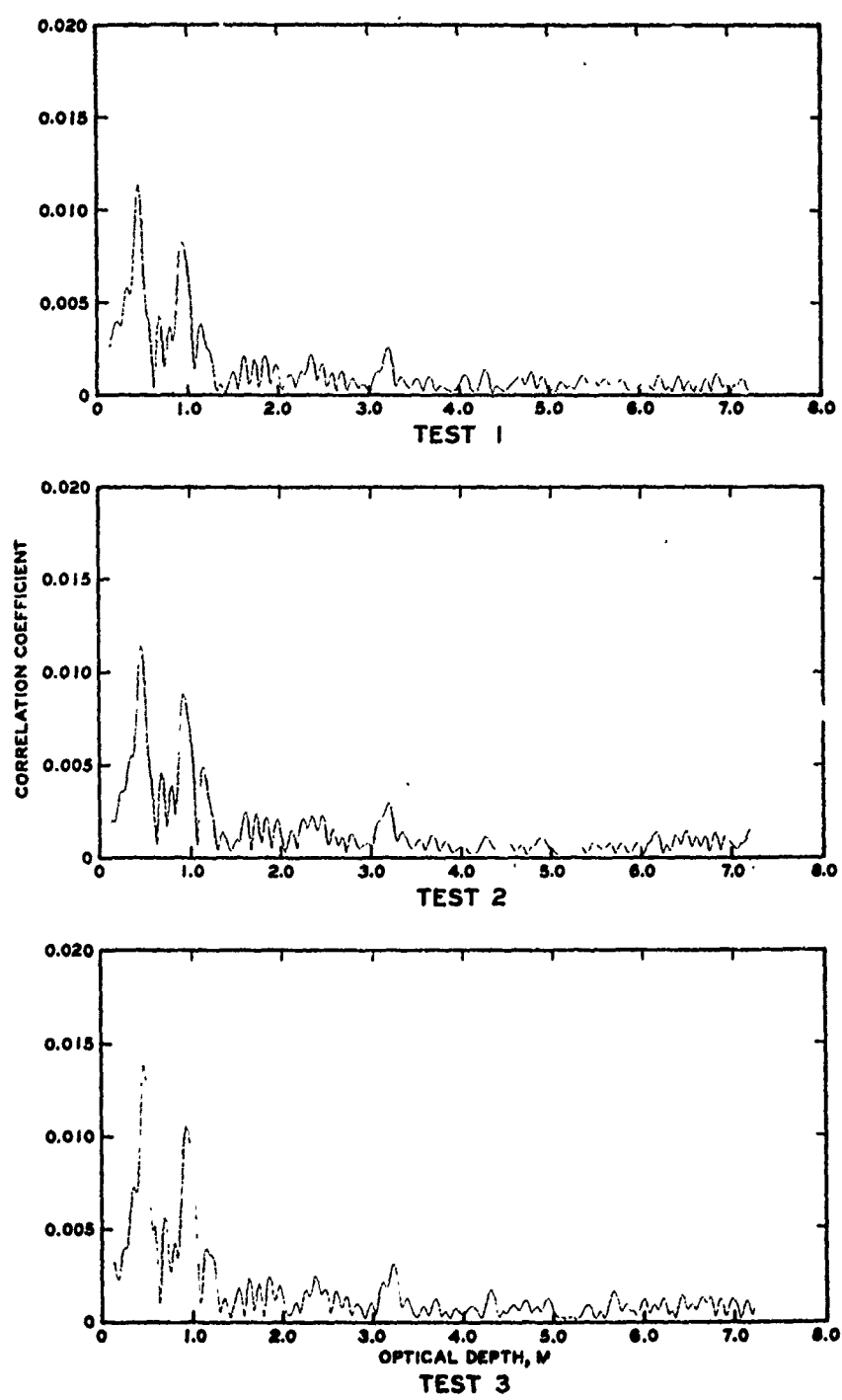


PLATE 8

50

POWER REFLECTANCE
VS
FREQUENCY
HIGHWAY TESTS
SITE 3 (STA 004)
TEST 9

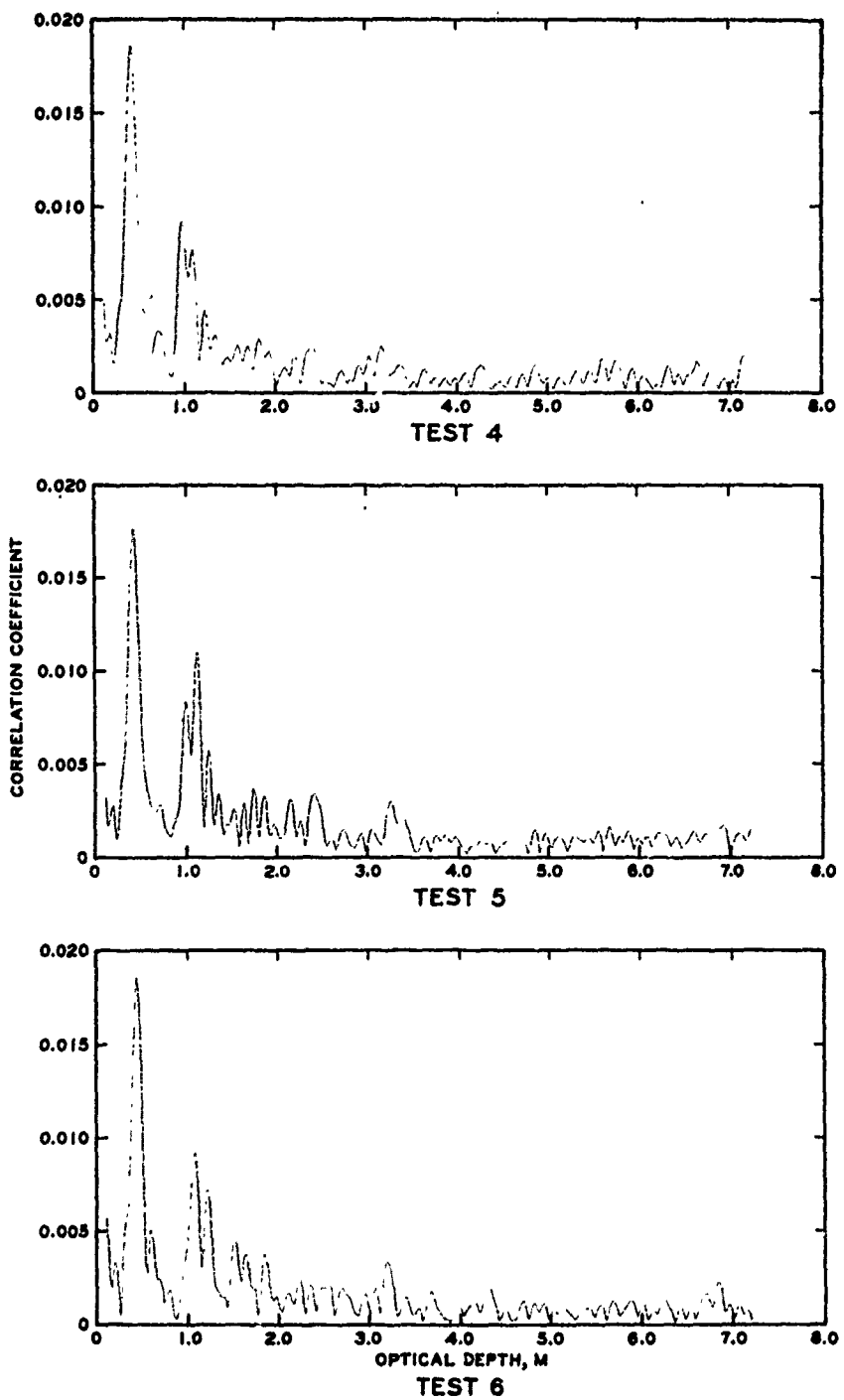




OPTICAL THICKNESS
HIGHWAY TESTS
SITE 1 (STA. 724)
TESTS 1, 2, AND 3

PLATE 10

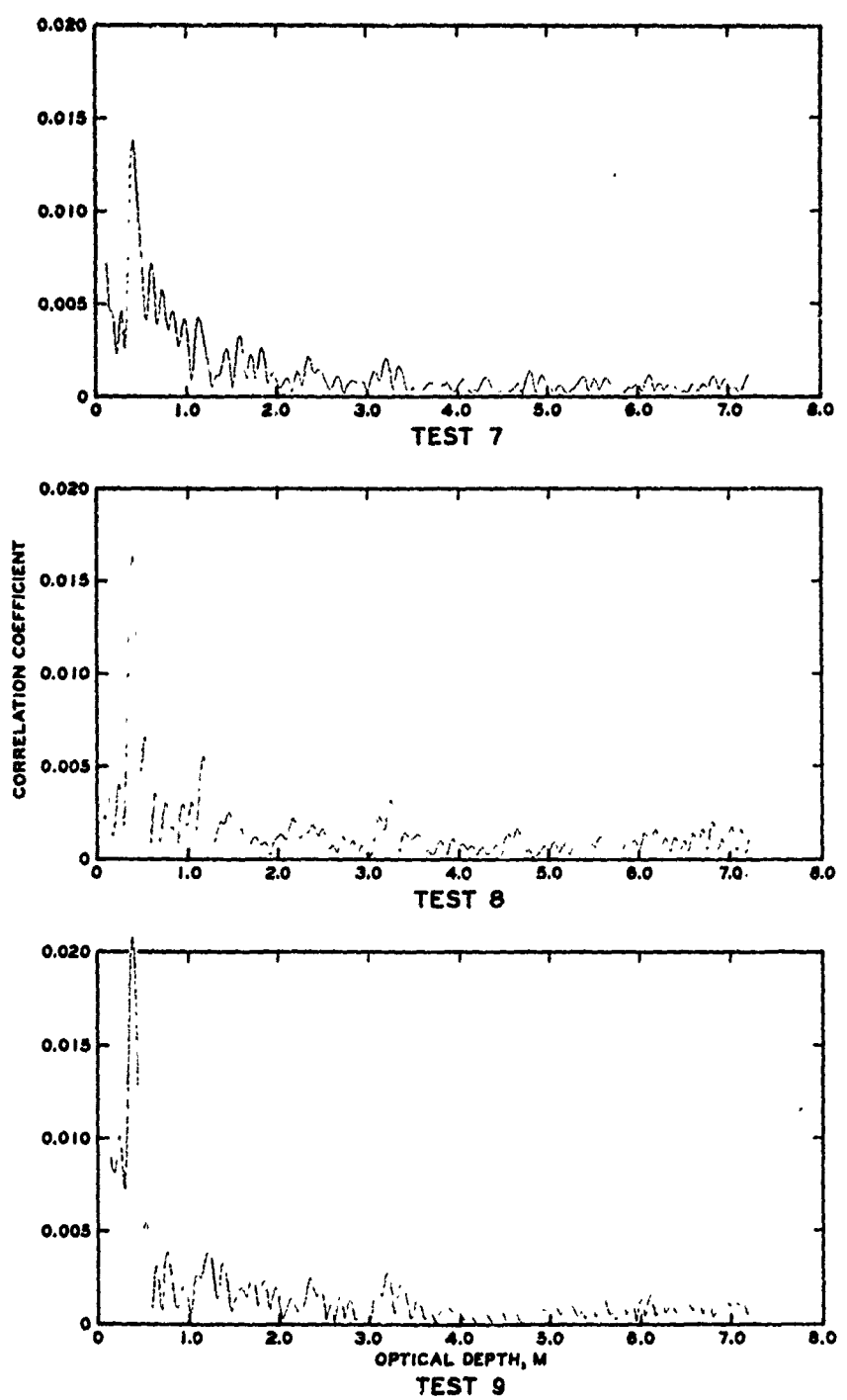
52



OPTICAL THICKNESS
HIGHWAY TESTS
SITE 2 (STA 654)
TESTS 4, 5, AND 6

53

PLATE II



OPTICAL THICKNESS
HIGHWAY TESTS
SITE 3 (STA 604)
TESTS 7, 8, AND 9

APPENDIX A: FOURIER TRANSFORM ANALYSIS

1. A periodic function with period T , defined by its values in the interval 0 to T , will have a Fourier expansion given by^{6*}

$$f(x) = \frac{1}{2} A_0 + \sum_{n=1}^{n=\infty} A_n \cos 2n\left(\frac{\pi}{T}\right)x + B_n \sin 2n\left(\frac{\pi}{T}\right)x \quad (A1)$$

or

$$f(x) = \frac{1}{2} C_0 + \sum_{n=1}^{n=\infty} C_n \cos (nx + \phi_n) \quad (A2)$$

where

$$A_n = \frac{2}{T} \int_0^T f(x) \cos \left(\frac{2n\pi x}{T}\right) dx \quad (A3)$$

$$B_n = \frac{2}{T} \int_0^T f(x) \sin \left(\frac{2n\pi x}{T}\right) dx \quad (A4)$$

and

$$C_0 = A_0$$

$$C_n = \left(A_n^2 + B_n^2 \right)^{1/2}$$

$$\phi_n = \tan^{-1} \left(\frac{-B_n}{A_n} \right)$$

for

$$n = 0, 1, 2, \dots$$

2. As shown in fig. A1, the points defined in the frequency domain will be $1/T$ apart.

3. If $f(x)$ is redefined so that the amplitude from T_1 to $2T_1$ is zero and the new period T_2 is twice as long as T_1 , the spacings between the points in the frequency domain will be reduced by half, and the amplitude of C_n for the points at $1/T_1$, $2/T_1$, $3/T_1$, ... frequency will be reduced by half (fig. A2).

4. This reduction can be seen in equations A3 and A4 for the Fourier coefficients. For example, from equation A3 for a period T_1 :

* Refers to corresponding listing in Literature Cited section following main text.

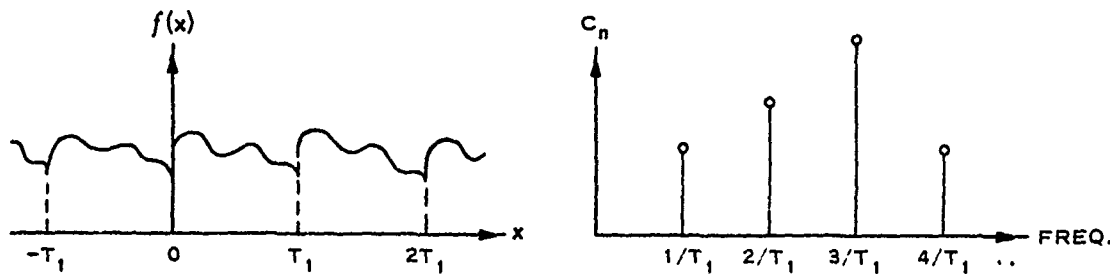


Fig. A1. Periodic wave and frequency function

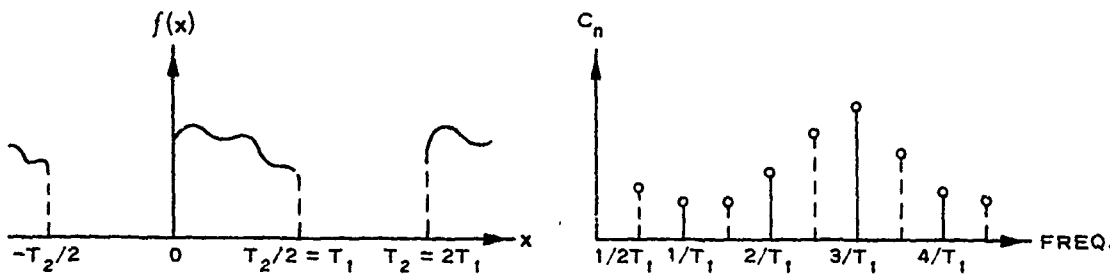


Fig. A2. Periodic wave and frequency function after adding zero-amplitude points

$$A_{n1} = \frac{2}{T_1} \int_0^{T_1} f_1(x) \cos\left(\frac{2n_1 \pi x}{T_1}\right) dx \quad (A5)$$

For a period of $T_2 = 2T_1$

$$A_{n2} = \frac{2}{T_2} \int_0^{T_2} f_2(x) \cos\left(\frac{2n_2 \pi x}{T_2}\right) dx \quad (A6)$$

$$A_{n2} = \frac{2}{2T_1} \int_0^{T_1} f_1(x) \cos\left(\frac{2n_2 \pi x}{2T_1}\right) dx + \frac{2}{2T_1} \int_{T_1}^{2T_1} f_2(x) \cos\left(\frac{2n_2 \pi x}{2T_1}\right) dx \quad (A7)$$

5. Since the function $f_2(x)$ is defined as zero between T_1 and $2T_1$, the second integral for A_{n2} in equation A7 is zero. The coefficients A_{n2} will be half of A_{n1} when $n_2/2$ is equal to n_1 because of the $2/T$ factor in front of the integral.

6. This same process can be generalized for the case of a function with an arbitrary fraction of its period at zero amplitude. The coefficients for the nonzero function can be written as

$$A_{nl} = \frac{T_2}{T_1} A_{n2} \quad (A8)$$

for

$$n_1 = n_2 \frac{T_1}{T_2}$$

7. The Fourier coefficients for A_{nl} for other than integral values of n_1 have some error because the function $f_2(x)$ can go to zero in the middle of a sine or cosine cycle. This effect can be reduced by subtracting the mean of $f_1(x)$ from each data point in $f_1(x)$ before calculating the Fourier transform.⁷ This has no effect on the A_{nl} values for integral values of n_1 . Also note that the values for A_{nl} for fractional values of n less than 1 have no meaning because the original data record $f_1(x)$ would not be as long as the sine or cosine period of the Fourier transform.